Stem Cell Reports
Report

ISSCR

OPEN ACCESS

High Levels of Canonical Wnt Signaling Lead to Loss of Stemness and Increased Differentiation in Hematopoietic Stem Cells

Farbod Famili,[1] Martijn H. Brugman,[1] Erdogan Taskesen,[2] Brigitta E.A. Naber,[1] Riccardo Fodde,[3] and Frank J.T. Staal[1,*]

[1]Department of Immunohematology and Blood Transfusion, Leiden University Medical Center, 2300 Leiden, the Netherlands
[2]Department of Clinical Genetics, VU University, 1081 Amsterdam, the Netherlands
[3]Department of Pathology, Erasmus Medical Center, 3000 Rotterdam, the Netherlands
*Correspondence: f.j.t.staal@lumc.nl
http://dx.doi.org/10.1016/j.stemcr.2016.04.009

SUMMARY

Canonical Wnt signaling regulates the self-renewal of most if not all stem cell systems. In the blood system, the role of Wnt signaling has been the subject of much debate but there is consensus that high Wnt signals lead to loss of reconstituting capacity. To better understand this phenomenon, we have taken advantage of a series of hypomorphic mutant *Apc* alleles resulting in a broad range of Wnt dosages in hematopoietic stem cells (HSCs) and performed whole-genome gene expression analyses. Gene expression profiling and functional studies show that HSCs with APC mutations lead to high Wnt levels, enhanced differentiation, and diminished proliferation but have no effect on apoptosis, collectively leading to loss of stemness. Thus, we provide mechanistic insight into the role of APC mutations and Wnt signaling in HSC biology. As Wnt signals are explored in various in vivo and ex vivo expansion protocols for HSCs, our findings also have clinical ramifications.

INTRODUCTION

In many tissues, including the blood, intestine and skin, old cells are eliminated and replenished by newly developed cells from a small pool of stem cells. This rare population of stem cells is located in a specific microenvironment, the niche, and gives rise to several different lineages of abundant daughter cells (Mendez-Ferrer et al., 2010). The signals controlling the various stem cell fates (self-renewal, differentiation, quiescence, apoptosis, and others) are beginning to be elucidated. A number of evolutionary conserved pathways are important for the development and maintenance of adult stem cells, including Notch, bone morphogenic protein, hedgehog, fibroblast growth factor, transforming growth factor β, and Wnt signals (Blank et al., 2008). Among these pathways, the Wnt pathway is seen as a dominant factor in self-renewal of many types of adult stem cells (Reya and Clevers, 2005). Compared with the convincing studies on the role of Wnt signaling in adult stem cells in skin and gut, a role for Wnt in adult hematopoietic stem cells (HSCs) has proved much more difficult to demonstrate (reviewed in Luis et al., 2012). In studies reporting an important role for Wnt signaling in blood cells, Wnt seemed to be required for normal HSC self-renewal and therefore for efficient reconstitution after transplantation (Luis et al., 2011).

Several types of Wnt signaling can be discerned often referred to as the canonical or Wnt/β-catenin pathway and the non-canonical pathways (reviewed extensively in Staal et al., 2008). In the absence of Wnt ligands, cytoplasmic levels of β-catenin are kept very low through the action of a protein complex (the so-called destruction complex) that actively targets β-catenin for degradation. This complex is composed of two negative regulatory kinases, including glycogen synthase kinase 3β (GSK-3β) and at least two anchor proteins that also function as tumor suppressor proteins, namely Axin1 or Axin2 and APC (adenomatous polyposis coli). APC and Axin function as negative regulators of the pathway by sequestering β-catenin in the cytoplasm. Hence, inactivating mutations in *Apc* lead to higher β-catenin protein accumulation among other important events controlled by APC. Activation of the pathway by Wnt leads to inactivation of the destruction complex allowing buildup of β-catenin and its migration to the nucleus. In the nucleus, β-catenin binds to members of the TCF/LEF transcription factor family, thereby converting them from transcriptional repressors into transcriptional activators.

Initial attempts to overexpress a constitutively active form of β-catenin in HSCs led to an increase in proliferation and repopulation capacity upon transplantation into lethally irradiated mice (Reya et al., 2003). However, later studies using conditional overexpression of a stabilized form of β-catenin led to a block in multilineage differentiation, and the exhaustion of long-term HSCs (Kirstetter et al., 2006; Scheller et al., 2006). This resulted in anemic mice and eventually led to lethality, i.e., the opposite effect when compared with the improved transplantation setting reported earlier. These studies have created confusion concerning the importance of Wnt in maintaining numbers and integrity of HSCs. Similarly, not all loss-of-function studies have produced clear phenotypes. The Mx-Cre

This is an open access article under the CC BY-NC-ND license (http://creativecommons.org/licenses/by-nc-nd/4.0/).

CrossMark

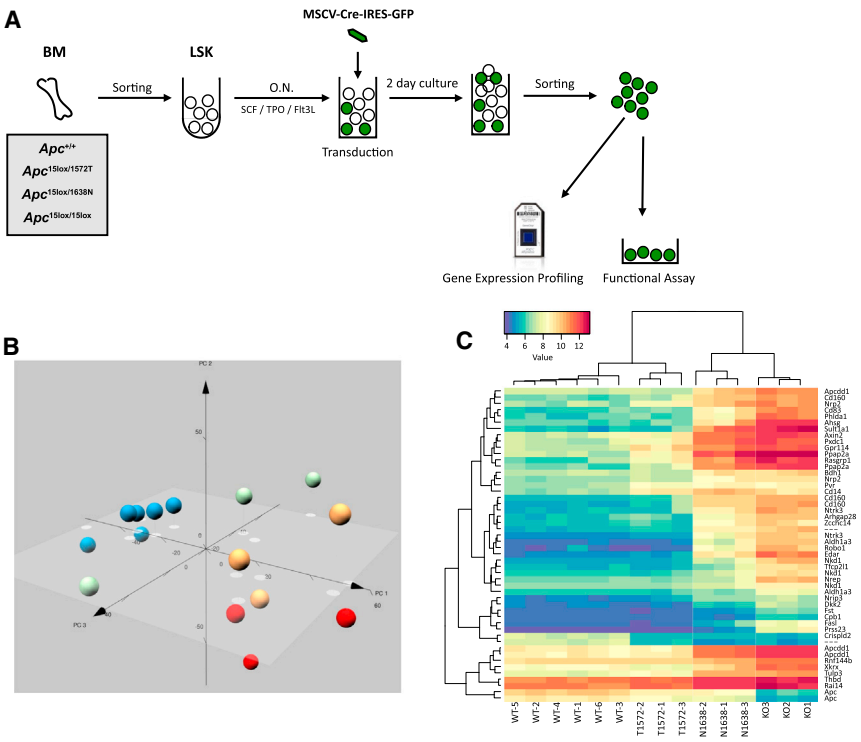

Figure 1. Definition of a High Wnt Stem Cell Signature

(A) Experimental setup. LSK cells from various APC mutant mice were sorted from bone marrow, transduced with Cre-GFP retrovirus and GFP-transduced cells were again sorted and used for further experiments.

(B) Principal component analysis plots of all 15 biological samples used in this study. The percentage of variance captured by each of the first three principal components is indicated.

(C) Hierarchical clustering of the various APC mutants and WT HSCs indicating the top 50 differentially expressed genes and changes in gene expression.

system has been used to drive deletion of β-catenin (Zhao et al., 2007) or both β-catenin and its homolog γ-catenin (Koch et al., 2008; Jeannet et al., 2008). However, no defects were reported in HSC function or cells within lymphoid tissues. Surprisingly, in vivo reporter assays revealed that the canonical Wnt signaling pathway was still active in HSCs despite the absence of both β- and γ-catenin (Jeannet et al., 2008). This could imply the existence of an alternative factor or generation of a hypomorphic allele permitting low levels of Wnt signaling that would negate hematopoietic defects. Heroic efforts to knock out the *Porcn* gene during hematopoiesis, which encodes an acyltransferase (porcupine) necessary for acylation of Wnts, enabling their secretion and binding to the frizzled receptors, have not resulted in hematopoietic defects; however, there also were no changes in Wnt signaling (Kabiri et al., 2015). The reasons for this are presently unknown, but incomplete deletion or the lack of need for Wnt secretion have been suggested (Oostendorp, 2015). This demonstrates the high complexity and difficulty in generating bona fide null mutants for canonical Wnts in the hematopoietic system. Together with studies in which Wnt activity in HSCs was reported to be close to zero (Fleming et al., 2008; Luis et al., 2009; Zhao et al., 2007), these findings suggest that complete absence of Wnt signaling is detrimental to HSC function, but that up to a quarter of normal activity is sufficient for normal function. Our recent findings suggest that these very different results in both gain-of-function and loss-of-function studies can be largely explained by differences in levels of Wnt signaling achieved in different experimental circumstances. That is, when Wnt signaling is slightly enhanced over normal levels, HSCs show improved reconstitution capacity. However, when HSCs express high levels of Wnt signaling, they completely fail to reconstitute irradiated recipient mice (Luis et al., 2011). Thus, different levels of activation of the pathway can account for the discrepancies in previous studies (Malhotra and Kincade, 2009).

RESULTS

Gene Expression Profiling and Correlation with Wnt Dosage

Previously, we have used a combination of two different hypomorphic alleles and a conditional deletion allele of the *Apc* gene resulting in a gradient of five distinct levels of Wnt signaling in vivo. In the *Apc*1572T and *Apc*1638N alleles, amino acid residues 1572 and 1638 have been targeted resulting in different levels and lengths of truncated Apc proteins, consequently leading to different levels of Wnt pathway activation. Deletion of *Apc* exon 15 within the Apc^{15lox} allele was performed ex vivo by using a Cre-recombinase encoding retrovirus (Figure 1A). LSK cells from wild-type (WT) mice ($Apc^{+/+}$) transduced with the same viral construct were employed as controls for all

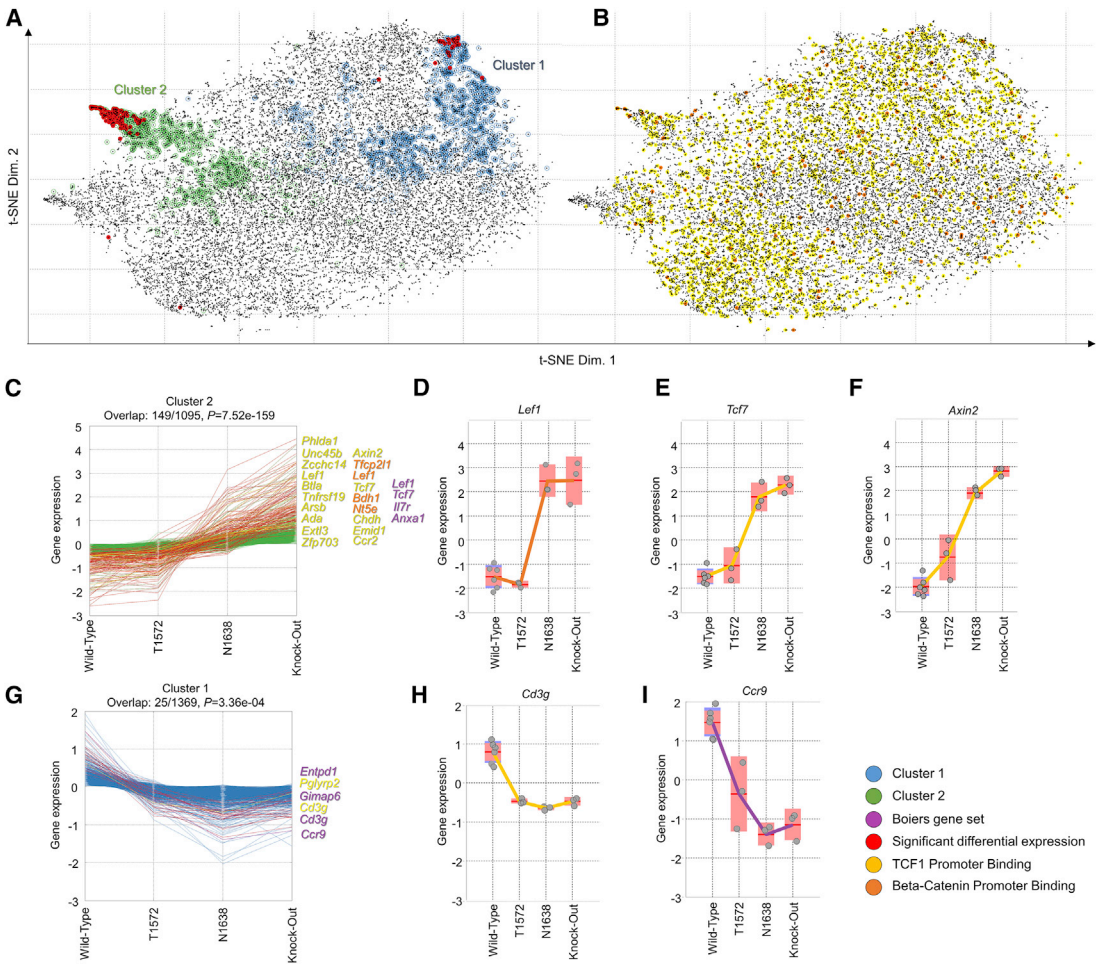

Figure 2. t-SNE Landscape of APC Mutants

(A and B) t-SNE maps of all probe sets. Red colored lines are differentially expressed genes, green are in cluster 15, yellow show both binding (TCF1/TCF7 or β-catenin), and differential expression. Text labels are shown only for the latter.

(C and G) Cluster 2 and 1 identified in t-SNE.

(D–F, H, and I) Selected genes with their expression in the various Apc mutants.

experiments. Transduced cells were sorted and employed for gene expression profiling by Affymetrix genome-wide microarrays. In the current report, we focused on the differences between WT LSK cells, which efficiently reconstitute recipient mice, and the LSK cells with increased Wnt signaling activity (*Apc*1572T, *Apc*1638N, and the Apc^{15lox} mutant alleles). Biological triplicates were used for each condition. As WT HSCs have low but detectable and slightly variable levels of Wnt signaling, and they form the basis for comparison of all other conditions, we used six replicates for WT HSCs.

Principal component analysis showed clear separation of the triplicate arrays per genotype corresponding to the different Wnt signaling levels (Figure 1B). Hierarchical clustering of the top 50 differentially expressed genes also revealed a clear separation of the different Wnt signaling clusters (Figure 1C).

Biological Processes Correlated with High Wnt Levels in HSC

Focusing on the most differentially expressed genes, a heatmap was constructed that clearly reveals the differences between WT and Apc^{15lox} HSCs (Figure 2A). We used the gene expression data of all available probe sets across the 15 APC samples and applied Barnes-Hut t-distributed stochastic neighbor embedding (t-SNE) to map each individual gene or probe set into a 2D space. The 2D landscape illustrates genes/probe sets with similar behavior (Figure 2B). Genes that have highly correlated expression profiles will be located in close proximity in the map, whereas uncorrelated expression profiles should be far apart in the t-SNE map. Genes that follow the increase in Wnt signaling cluster in a set of genes composed of known Wnt target genes, such as *Axin2, Tcf7*, and *Lef1* (Figures 2C–2F). Genes that

are anti-correlated with increased Wnt signaling can also be discerned and include *Ccr9* and *Cd3g* (Figures 2G–2I).

The differential gene expression as detected by microarray analysis was validated using digital Q-PCR (Figure S1A). Checking the biological processes involved in the differences between low and high Wnt signaling, we observed gene sets found in Wnt and Notch signaling but also differentiation into monocytes, myeloid cells, and B lymphocytes (Figure S1B). No differences were observed in apoptosis or cell-cycle-related genes. We confirmed these findings by specifically selecting published gene sets for these processes and checking whether clustering with the published gene sets correlated with the Apc mutants. The differentially expressed genes we found were highly enriched in the B lymphoid and myeloid differentiation signatures but not for pro-apoptotic or anti-apoptotic genes (Figures S1B, S2, and S3).

Apc Mutants Causing High Levels of Wnt Signaling Inhibit Proliferation but Do Not Change Apoptosis

Ming et al. (2012) reported that HSCs with high Wnt signals have increased apoptosis due to a high level of Wnt signaling and impaired self-renewal in HSCs. In their study, an activated form of β-catenin was used resulting in increased Wnt signaling in HSCs to the same level as the *Apc*1638N mutant used here. We therefore also used a constitutively active β-catenin conditional allele targeted the same way as the conditional 15lox APC$^{-/-}$ LSK cells to check the *Axin2* levels as readout for the Wnt signaling dosage. The β-catenin (ΔEx3) allele (Harada et al., 1999) gave 21-fold higher *Axin2* levels in LSK cells compared with WT LSK cells transduced with GFP-Cre, whereas the 1638N resulted in 23-fold and the Apc15lox ~50-fold higher *Axin2* mRNA levels. Thus, the *Axin2* levels and hence activation of the Wnt pathway were similar. However, our gene expression analysis did not show any significant differentially expressed genes associated with apoptosis. In order to study the putative involvement of apoptosis with a more functional approach, we performed two different apoptosis assays. First, we assessed apoptosis by annexin V/7-amino-actinomycin (7-AAD) staining of the ex vivo transduced LSK cells from *Apc* WT and *Apc*$^{15lox/15lox}$ (Figure 3A). At the beginning of culture, there was almost no apoptosis in both groups (~4% at day 0). After 3 days of culture, the percentage of annexin V^{+} apoptotic cells increased to ~16%. However, no difference was observed between the *Apc* WT and knockout (KO) groups. Next, we performed caspase-3 staining in order to assess the apoptosis rate of ex vivo transduced LSK cells (Figure 3B). Similar to previous assays, there was hardly any caspase-3 positivity at the beginning of the culture, while it was elevated after 3 days of culture. However, again no difference was observed between the two groups. Subsequently, we analyzed the proliferation status of the transduced LSK cells by labeling the cells with proliferation dye EF670 (Figure 3C). While cells did not proliferate at the beginning of culture (filled gray histogram), *Apc* WT LSK cells proliferated around 4-fold more than *Apc* KO LSK cells. Therefore, although a high level of Wnt signaling does not affect apoptosis, it decreases proliferation of LSK cells after 3 days of culture.

High Wnt HSCs Show Enhanced Myeloid and B Lymphoid Differentiation Capacity

Our gene expression analysis revealed that LSK cells with high levels of Wnt induce upregulation of B and myeloid-associated genes (Figure S2). In order to confirm this observation functionally, we performed in vitro B and myeloid differentiation assays using the OP9 stromal cell line (Figure 4). LSK cells were sorted, transduced with the Cre-GFP retrovirus, and cultured for 14 days on OP9 cells. *Apc* lox15 LSK cells developed to granulocytes (CD11b^{+} Gr1^{+}) with around 2-fold higher frequency, and developed to B cell lineage (B220^{+} CD19^{+}) with around 2.5-fold higher frequency compared with WT LSK cells. Thus, we confirmed by functional assays that *Apc* mutations leading to a high level of Wnt signaling enhance differentiation toward B and myeloid lineages.

DISCUSSION

The Wnt signaling pathway has emerged as the dominant self-renewal pathway for various adult-type stem cells and is required for maintenance of embryonic as well as induced pluripotent stem cells. In the hematopoietic system, only mild increased Wnt dosages result in higher stem cell activity; indeed the overall Wnt signaling levels in HSC are much lower than those found in intestinal, skin, or mammary gland stem cells. Nevertheless, complete loss of Wnt signaling leads to defective self-renewal as shown in secondary transplantations. This had led to interest in the use of Wnt signaling or factors that modulate Wnt signaling, such as prostaglandin E2 (PGE2) (Goessling et al., 2009) or GSK-3β inhibitors (Huang et al., 2012), for expansion of HSCs ex vivo.

We previously demonstrated that Wnt signaling functions in a strictly controlled dosage-dependent fashion (Luis et al., 2011). As also shown by several other laboratories (Kirstetter et al., 2006; Ming et al., 2012) (Scheller et al., 2006), high Wnt levels in HSCs eventually lead to stem cell exhaustion and lack of reconstitution of irradiated recipients. In the current study, we used gene expression profiling to understand why *Apc* mutations that lead to high Wnt signaling (among other defects) in HSCs would lead to loss of repopulating capacity. Our results

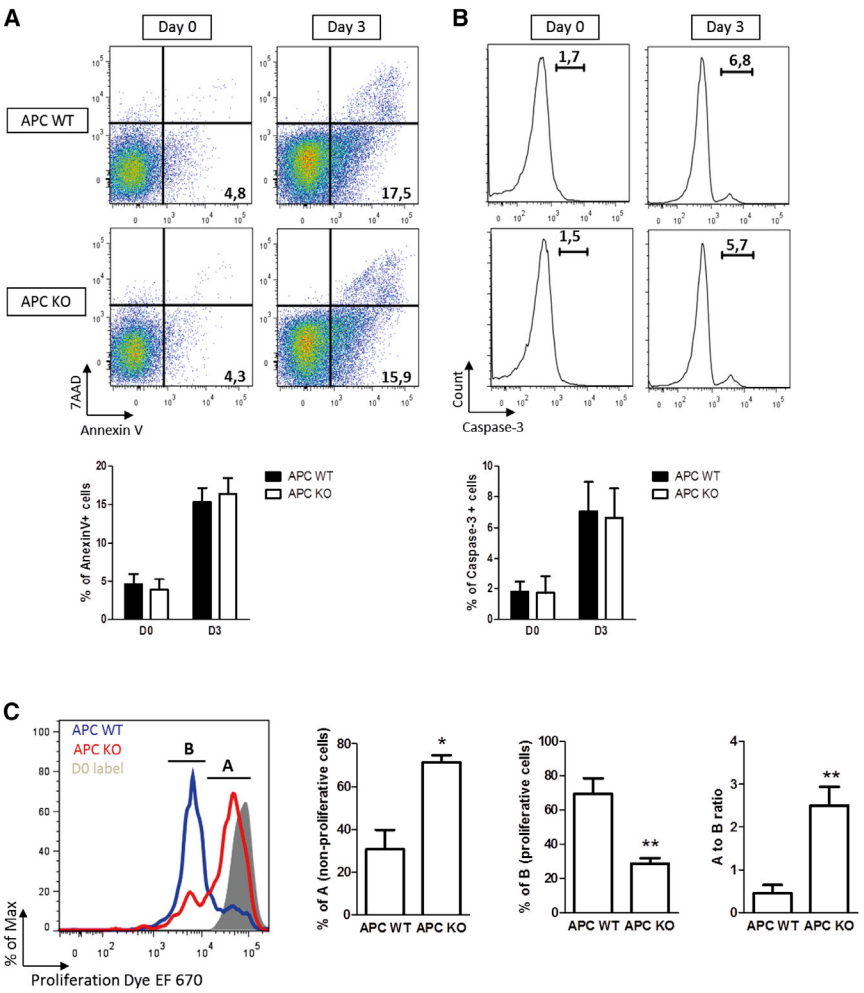

Figure 3. High Levels of Wnt Signaling Do Not Affect Apoptosis

(A and B) Sorted BM LSK from Apc WT and 15lox/15lox were transduced with Cre virus and cultured for 2 days to fulfill Cre recombination activity. After culturing for 2 days (day 0) and 5 days (day 3), cells were harvested and stained with annexin V/7-AAD (left graph) or active caspase-3 (right graph). Error bars represent the SD of three replicates of one independent experiment.

(C) Sorted BM LSK from Apc WT and 15lox/15lox were transduced with Cre virus, cultured for 2 days and labeled with 5 μM proliferation dye EF670 or with DMSO. The left plot depicts representative histogram plots and the right graphs show the percentage of non-proliferative cells (A), proliferative cells (B), and ratio of A/B. Error bars represent the SD of three samples from individual mice in one independent experiment. Two independent experiments were done with similar outcome. *$p < 0.05$ and **$p < 0.01$ (Mann-Whitney U test).

show, both at the genetic level and in functional assays, increased differentiation, diminished proliferation, and no effects on apoptosis. The much stronger differentiation toward mature blood linages coupled with loss of HSC proliferation (see also Figure S4) is expected to lead to lower reconstitution by HSCs. Collectively, these data explain the lack of maintaining bona fide stemness in *Apc* exon 15 deleted HSCs. Thus, instead of increased apoptosis of HSCs, here we offer another explanation for the loss of reconstitution capacity induced by high Wnt levels.

An alternative interpretation of our data is that the observed consequences of *Apc* mutant alleles are not Wnt but rather APC dependent. *Apc* encodes for a multifunctional protein involved in a broad spectrum of cellular functions (Gaspar and Fodde, 2004). To date, most *Apc* mutant mouse models are characterized by tumor phenotypes that depend completely on Wnt dosage. Apc1638T, the only targeted *Apc* mutation that does not affect Wnt signaling at all, results in homozygous viable and tumor-free animals, notwithstanding the deletion of the C-terminal third of the protein containing many functional domains (Smits et al., 1999, 2000). Deletion of only a few amino acids encompassing crucial Axin-binding motifs results in Wnt signaling activation, tumor formation, and lack of reconstitution by HSCs, as we have shown before (Luis et al., 2011). Finally, mutations affecting other members of the Wnt pathway, such as Gsk3β and β-catenin, result in levels of signaling activation and hematopoietic defects that are fully in agreement with our results (Goessling et al., 2009; Huang et al., 2009, 2012; Lane et al., 2010). Therefore, the most likely explanation is that specific levels of Wnt signaling are the major determinant of the observed differential effects on hematopoiesis. In addition, recent studies using recombinant Wnt3a also showed a dose-dependent effect on HSC biology (Famili et al., 2015) where high Wnt3a leads to loss of human HSC proliferation in vitro (Duinhouwer et al., 2015), underscoring the differential effects we also have observed with the different *Apc* alleles and correlating exactly with the Wnt dosages caused by these mutations.

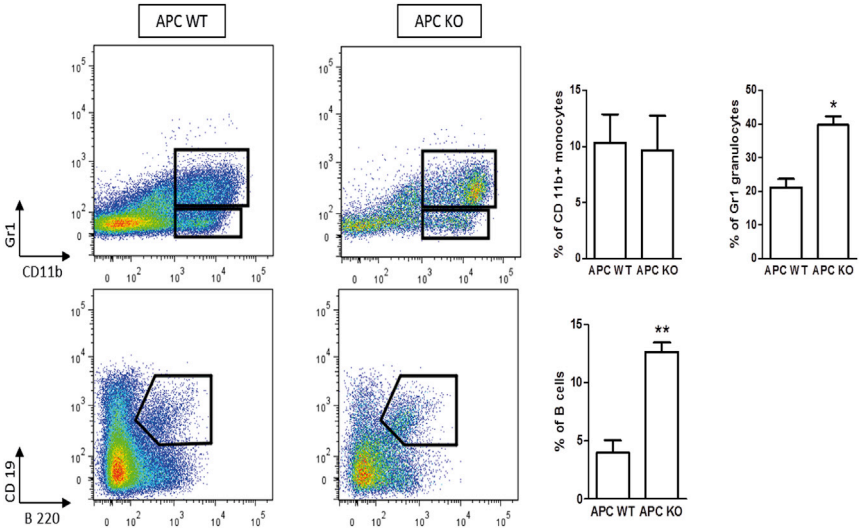

Figure 4. High Levels of Wnt Signaling Enhances Multilineage Differentiation

Transduced LSK cells from Apc WT and 15lox/15lox were co-cultured with OP9 stromal cell line for 14 days, then were harvested, and assessed by flow cytometry for myeloid (CD11b and Gr1$^+$) and B cell development (B220 and CD19$^+$). Error bars represent the SD of six samples from individual mice from two independent experiments. Asterisks indicate statistical significance as follows: *$p < 0.05$, and **$p < 0.01$ (Mann-Whitney U test).

The finding that the *Apc* 15lox mutant leading to high Wnt signaling levels is associated with increased numbers of differentiated cells is not unprecedented. In the intestine, Wnt signaling induces maturation of Paneth cells that contain active β-catenin and Tcf4 (van Es et al., 2005), confirming that high Wnt signaling levels can drive differentiation processes.

Other investigators have used a different system to increase Wnt signals in HSCs, namely overexpression of an oncogenic, constitutively active form of β-catenin (Ming et al., 2012). They showed an increase in apoptosis using annexin V/propidium iodide staining from 10% in WT LSK cells to 35% in high Wnt LSK cells. The reasons for the differences with our results could be due to differences in the systems used, although both are expected to lead to high Wnt signaling levels. Possibly activated β-catenin also negatively affects cell adhesion and homing properties thereby decreasing exposure to important survival signals leading to increased apoptosis. It is also noteworthy that enhanced survival signals are needed to have HSCs survive in the oncogenic β-catenin system. In addition, Li et al. (2013) have shown that Apc regulates the function of HSCs largely through β-catenin-dependent mechanisms, thus demonstrating that, in both systems, canonical Wnt signaling is the major factor.

Whatever the exact mechanism, it is clear that Wnt signaling levels need to be strictly controlled. It is well possible that somewhat higher Wnt levels, which are detrimental to stemness, can be tolerated if HSC survival is enhanced, which then would lead to better self-renewal at this somewhat higher Wnt signaling dose. For instance PI3K/Akt signaling (Perry et al., 2011), as well as expression of Bcl2 (Reya et al., 2003) can provide such signals. Apparently, high Wnt signaling levels can be tolerated in HSC in combination with activation of other survival pathways. Intriguingly, the high Wnt levels in combination with oncogene activation in acute myeloid leukemia seem to allow the Wnt pathway to function as a self-renewal factor for leukemic stem cells (Wang et al., 2010), whereas high Wnt levels cannot do so in normal HSCs. The different localization of normal versus malignant HSCs in the bone marrow niche (Lane et al., 2011) may also contribute to this differential outcome of high Wnt dosage and opens up a therapeutic window targeting leukemic but not normal stem cells.

EXPERIMENTAL PROCEDURES

Mice

Mice were bred and maintained in the animal facilities of Leiden University Medical Center, in accordance with legal regulations in the Netherlands and with the approval of the Dutch animal ethical committee.

Microarray Analysis

In this study, we measured the genome-wide gene expression profiles in 21 APC C57Bl/6 mouse samples using Affymetrix mouse 430 2 microarrays for four different conditions; six APC WT, three APC 15lox/1572T, three APC 15lox/1638N, and three APC 15lox/15lox mice. 40,000–70,000 sorted LSK cells were stimulated overnight in serum-free medium (STEMCELL Technologies) supplemented with cytokines and transduced by spinoculation with MSCV-Cre-IRES-GFP. Subsequently, Cre-GFP-expressing LSK cells were isolated using flow cytometric cell sorting and collected for RNA expression. RNA of more than 10,000 cells was amplified and processed using the Encore Biotin module and hybridized to Affymetrix mouse 430 2.0 Genechip arrays. Differential expressed genes were determined using Limma, and genes were considered to be differentially expressed if mRNA levels differ with $p \leq 0.05$ after multiple test correction using Holm.

The dataset associated with this study has been deposited at GEO: GSE79495.

Flow Cytometry

Cells were stained in fluorescence-activated cell sorting buffer at 4°C, washed, and measured either on a Canto I or an Aria (BD Biosciences). Data were analyzed using FlowJo software (Tree Star).

Proliferation, Apoptosis, and Differentiation Assays

For apoptosis, cells were harvested after 2 days (day 0) or 5 days (day 3) of culture, and stained with either 7-AAD/annexin V (BD Bioscience), or phycoerythrin-active caspase-3 apoptosis kit (BD Pharmingen). For the proliferation assay, cells were labeled with 5 μM Cell Proliferation Dye eFluor 670 (eBioscience) at day 0. Subsequently, cells were harvested at day 3 and were assessed for proliferation. For differentiation assays, LSK cells were transduced at day 0 and transferred onto confluent monolayers of OP9 WT. After 14 days, cells were harvested and assessed by flow cytometry for B and myeloid lineage differentiation.

SUPPLEMENTAL INFORMATION

Supplemental Information includes Supplemental Experimental Procedures, four figures, and three tables and can be found with this article online at http://dx.doi.org/10.1016/j.stemcr.2016.04.009.

ACKNOWLEDGMENTS

We thank Edwin de Haas for expert cell sorting and Paul Roozen for initiating this project. We thank Bjorn Clausen for help with the constitutive activated β-catenin allele. This work was supported in part by a TOP grant from The Netherlands Organization for Health Research and Development (ZonMw Project 40-00812-98-09050), a grant from the Dutch government to the Netherlands Institute for Regenerative Medicine (NIRM, grant no. FES0908), and JSH/EHA fellowship to M.H.B.

Received: October 22, 2015
Revised: April 7, 2016
Accepted: April 11, 2016
Published: May 10, 2016

REFERENCES

Blank, U., Karlsson, G., and Karlsson, S. (2008). Signaling pathways governing stem-cell fate. Blood *111*, 492–503.

Duinhouwer, L.E., Tuysuz, N., Rombouts, E.W., Ter Borg, M.N., Mastrobattista, E., Spanholtz, J., Cornelissen, J.J., Ten Berge, D., and Braakman, E. (2015). Wnt3a protein reduces growth factor-driven expansion of human hematopoietic stem and progenitor cells in serum-free cultures. PLoS One *10*, e0119086.

Famili, F., Naber, B.A., Vloemans, S., De Haas, E.F., Tiemessen, M.M., and Staal, F.J. (2015). Discrete roles of canonical and non-canonical Wnt signaling in hematopoiesis and lymphopoiesis. Cell Death Dis. *6*, e1981.

Fleming, H.E., Janzen, V., Lo Celso, C., Guo, J., Leahy, K.M., Kronenberg, H.M., and Scadden, D.T. (2008). Wnt signaling in the niche enforces hematopoietic stem cell quiescence and is necessary to preserve self-renewal in vivo. Cell Stem Cell *2*, 274–283.

Gaspar, C., and Fodde, R. (2004). APC dosage effects in tumorigenesis and stem cell differentiation. Int. J. Dev. Biol. *48*, 377–386.

Goessling, W., North, T.E., Loewer, S., Lord, A.M., Lee, S., Stoick-Cooper, C.L., Weidinger, G., Puder, M., Daley, G.Q., Moon, R.T., et al. (2009). Genetic interaction of PGE2 and Wnt signaling regulates developmental specification of stem cells and regeneration. Cell *136*, 1136–1147.

Harada, N., Tamai, Y., Ishikawa, T., Sauer, B., Takaku, K., Oshima, M., and Taketo, M.M. (1999). Intestinal polyposis in mice with a dominant stable mutation of the beta-catenin gene. EMBO J. *18*, 5931–5942.

Huang, J., Zhang, Y., Bersenev, A., O'Brien, W.T., Tong, W., Emerson, S.G., and Klein, P.S. (2009). Pivotal role for glycogen synthase kinase-3 in hematopoietic stem cell homeostasis in mice. J. Clin. Invest. *119*, 3519–3529.

Huang, J., Nguyen-McCarty, M., Hexner, E.O., Danet-Desnoyers, G., and Klein, P.S. (2012). Maintenance of hematopoietic stem cells through regulation of Wnt and mTOR pathways. Nat. Med. *18*, 1778–1785.

Jeannet, G., Scheller, M., Scarpellino, L., Duboux, S., Gardiol, N., Back, J., Kuttler, F., Malanchi, I., Birchmeier, W., Leutz, A., et al. (2008). Long-term, multilineage hematopoiesis occurs in the combined absence of beta-catenin and gamma-catenin. Blood *111*, 142–149.

Kabiri, Z., Numata, A., Kawasaki, A., Edison, Tenen, D.G., and Virshup, D.M. (2015). Wnts are dispensable for differentiation and self-renewal of adult murine hematopoietic stem cells. Blood *126*, 1086–1094.

Kirstetter, P., Anderson, K., Porse, B.T., Jacobsen, S.E., and Nerlov, C. (2006). Activation of the canonical Wnt pathway leads to loss of hematopoietic stem cell repopulation and multilineage differentiation block. Nat. Immunol. *7*, 1048–1056.

Koch, U., Wilson, A., Cobas, M., Kemler, R., Macdonald, H.R., and Radtke, F. (2008). Simultaneous loss of - and {gamma}-catenin does not perturb hematopoiesis or lymphopoiesis. Blood *111*, 160–164.

Lane, S.W., Sykes, S.M., Al-Shahrour, F., Shterental, S., Paktinat, M., Lo Celso, C., Jesneck, J.L., Ebert, B.L., Williams, D.A., and Gilliland, D.G. (2010). The Apc(min) mouse has altered hematopoietic stem cell function and provides a model for MPD/MDS. Blood *115*, 3489–3497.

Lane, S.W., Wang, Y.J., Lo Celso, C., Ragu, C., Bullinger, L., Sykes, S.M., Ferraro, F., Shterental, S., Lin, C.P., Gilliland, D.G., et al. (2011). Differential niche and Wnt requirements during acute myeloid leukemia progression. Blood *118*, 2849–2856.

Li, W., Hou, Y., Ming, M., Yu, L., Seba, A., and Qian, Z. (2013). Apc regulates the function of hematopoietic stem cells largely through beta-catenin-dependent mechanisms. Blood *121*, 4063–4072.

Luis, T.C., Weerkamp, F., Naber, B.A., Baert, M.R., de Haas, E.F., Nikolic, T., Heuvelmans, S., De Krijger, R.R., van Dongen, J.J., and Staal, F.J. (2009). Wnt3a deficiency irreversibly impairs hematopoietic stem cell self-renewal and leads to defects in progenitor cell differentiation. Blood *113*, 546–554.

Luis, T.C., Naber, B.A., Roozen, P.P., Brugman, M.H., de Haas, E.F., Ghazvini, M., Fibbe, W.E., van Dongen, J.J., Fodde, R., and Staal, F.J. (2011). Canonical wnt signaling regulates hematopoiesis in a dosage-dependent fashion. Cell Stem Cell *9*, 345–356.

Luis, T.C., Ichii, M., Brugman, M.H., Kincade, P., and Staal, F.J. (2012). Wnt signaling strength regulates normal hematopoiesis and its deregulation is involved in leukemia development. Leukemia *26*, 414–421.

Malhotra, S., and Kincade, P.W. (2009). Wnt-related molecules and signaling pathway equilibrium in hematopoiesis. Cell Stem Cell *4*, 27–36.

Mendez-Ferrer, S., Michurina, T.V., Ferraro, F., Mazloom, A.R., Macarthur, B.D., Lira, S.A., Scadden, D.T., Ma'ayan, A., Enikolopov, G.N., and Frenette, P.S. (2010). Mesenchymal and haematopoietic stem cells form a unique bone marrow niche. Nature *466*, 829–834.

Ming, M., Wang, S., Wu, W., Senyuk, V., Le Beau, M.M., Nucifora, G., and Qian, Z. (2012). Activation of Wnt/beta-catenin protein signaling induces mitochondria-mediated apoptosis in hematopoietic progenitor cells. J. Biol. Chem. *287*, 22683–22690.

Oostendorp, R.A. (2015). Secretion of Wnts is dispensable for hematopoiesis. Blood *126*, 1051–1052.

Perry, J.M., He, X.C., Sugimura, R., Grindley, J.C., Haug, J.S., Ding, S., and Li, L. (2011). Cooperation between both Wnt/{beta}-catenin and PTEN/PI3K/Akt signaling promotes primitive hematopoietic stem cell self-renewal and expansion. Genes Dev. *25*, 1928–1942.

Reya, T., and Clevers, H. (2005). Wnt signalling in stem cells and cancer. Nature *434*, 843–850.

Reya, T., Duncan, A.W., Ailles, L., Domen, J., Scherer, D.C., Willert, K., Hintz, L., Nusse, R., and Weissman, I.L. (2003). A role for Wnt signalling in self-renewal of haematopoietic stem cells. Nature *423*, 409–414.

Scheller, M., Huelsken, J., Rosenbauer, F., Taketo, M.M., Birchmeier, W., Tenen, D.G., and Leutz, A. (2006). Hematopoietic stem cell and multilineage defects generated by constitutive beta-catenin activation. Nat. Immunol. *7*, 1037–1047.

Smits, R., Kielman, M.F., Breukel, C., Zurcher, C., Neufeld, K., Jagmohan-Changur, S., Hofland, N., van Dijk, J., White, R., Edelmann, W., et al. (1999). Apc1638T: a mouse model delineating critical domains of the adenomatous polyposis coli protein involved in tumorigenesis and development. Genes Dev. *13*, 1309–1321.

Smits, R., Hofland, N., Edelmann, W., Geugien, M., Jagmohan-Changur, S., Albuquerque, C., Breukel, C., Kucherlapati, R., Kielman, M.F., and Fodde, R. (2000). Somatic Apc mutations are selected upon their capacity to inactivate the beta-catenin downregulating activity. Genes Chromosomes Cancer *29*, 229–239.

Staal, F.J., Luis, T.C., and Tiemessen, M.M. (2008). WNT signalling in the immune system: WNT is spreading its wings. Nat. Rev. Immunol. *8*, 581–593.

van Es, J.H., Jay, P., Gregorieff, A., van Gijn, M.E., Jonkheer, S., Hatzis, P., Thiele, A., van den Born, M., Begthel, H., Brabletz, T., et al. (2005). Wnt signalling induces maturation of Paneth cells in intestinal crypts. Nat. Cell Biol. *7*, 381–386.

Wang, Y., Krivtsov, A.V., Sinha, A.U., North, T.E., Goessling, W., Feng, Z., Zon, L.I., and Armstrong, S.A. (2010). The Wnt/beta-catenin pathway is required for the development of leukemia stem cells in AML. Science *327*, 1650–1653.

Zhao, C., Blum, J., Chen, A., Kwon, H.Y., Jung, S.H., Cook, J.M., Lagoo, A., and Reya, T. (2007). Loss of beta-catenin impairs the renewal of normal and CML stem cells in vivo. Cancer Cell *12*, 528–541.

Stem Cell Reports, Volume *6*

Supplemental Information

High Levels of Canonical Wnt Signaling Lead to Loss of Stemness and Increased Differentiation in Hematopoietic Stem Cells

Farbod Famili, Martijn H. Brugman, Erdogan Taskesen, Brigitta E.A. Naber, Riccardo Fodde, and Frank J.T. Staal

Supplementary Experimental Procedures

High levels of canonical Wnt signaling lead to loss of stemness and increased differentiation in hematopoietic stem cells.

Farbod Famili, Martijn H. Brugman, Erdogan Taskesen, Brigitta E.A. Naber, Riccardo Fodde, Frank J.T. Staal

Supplemental Experimental procedures

Mouse bone marrow (BM) cells were isolated from femurs and tibiae, which were crushed in a mortar and filtered through 70 µm filters. The cells were stained using biotinylated lineage antibodies (MAC-1/CD11b, B220/CD45R, CD3e, CD4, NK1.1, Gr1, Ter119), Streptavidin PE, CD117 APC and Sca1 PECy7. LSK cells were isolated using a BD Aria II SORP cell sorter (Beckton-Dickinson) and were collected in Stemspan (Stem Cell Technologies), supplemented with mFlt3L (50 ng/ml), rmSCF (100 ng/ml) and rmTPO (10 ng/ml, all cytokines purchased from R&D sytems. The cells were incubated for 16 hr at 37°C and 5% CO_2. LSKs from Apc 15 Lox heterozygous mice with mildly elevated Wnt levels were shown to perform better in reconstitution experiments but are not integral part of the current study, as only subtle changes in gene expression were found.

Retroviral Production and Transduction

MSCV-Cre-IRES-GFP plasmid was kindly provided by H. Nakauchi (Institute of Medical Science, University of Tokyo, Japan) and viruses were generated with the Phoenix-packaging cell line. 40,000–70,000 sorted LSKs were stimulated overnight in serum-free medium (StemCell Technologies) supplemented with cytokines (100 ng/ml rmSCF, 10 ng/ml rmTPO, and 50 ng/ml rmFlt3L; from R&D) and transduced by spinoculation (800 x g, 2 hours, 32°C) with titrated amounts of virus with Retronectin (Takara Bio Inc.). Cells were cultured for 2 additional days. Subsequently, Cre-GFP expressing LSK cells were isolated using flow cytometic cell sorting and collected for RNA expression. For in vitro assays including apoptosis, proliferation and differentiation assays bulk of transduced and untransduced cells were used.

RNA amplification

RNA was isolated from the sorted transduced cells using Qiagen RNEasy micro columns (Qiagen, Hilden, Germany). RNA of more than 10,000 cells were then amplified using the Ovation RNA amplification system v2(Nugen Inc., San Carlos, CA, USA), processed using the Encore Biotin module (Nugen) and hybridized to Affymetrix mouse 430 2.0 Genechip arrays.
Data is available at the NCBI Gene Expression Omnibus (GEO), accession number GSE79495

Gene expression normalization. Gene expression data was measured in two batches. Raw data is normalized per batch with Robust Multi-Array Average (RMA), and batch correction is applied using Combat. Intensity values were mean centered per probe set. Gene symbols are mapped using MM9. As a result of the normalization, probe-intensity values follow a normal distribution for which intensities higher than 0 are up-regulated, and intensities lower than 0 are down-regulated. Principal component analysis and pairwise correlations across the 21 samples showed the expected results; wild-type and mutants, t1572, n1638, and Knock-Out samples are different from each other in the PCA-space and correlation map.

Gene expression analysis. Differential expressed genes for the APC samples are determined by using Limma, and genes are considered to be differential expressed between the two selected groups if mRNA levels differ with $P \leq 0.05$ after multiple test correction using Holm.

ChIP-Seq normalization. In this study we used massively parallel sequenced DNA-fragments bound by the transcription factors, TCF1, TCF7, and β-catenin. All the sequencing data is aligned using Burrows-Wheeler transformation (BWA), according MM9. We used several literature sources (Li et al., 2013a; Steinke et al., 2014; Zhang and Li, 2008; Zhang et al., 2000) (Wu et al., 2012).

ChIP-Seq analysis. Binding of transcription factors is determined by utilizing Hypergeometric Analysis of Tilling arrays (HATSEQ). A binding event was called when fragments are enriched based on default parameter settings, i.e., FWER significance level < 0.05, and a bandwidth (fragment size) of 300bp. We mapped the significantly detected binding sites to RefSeq genes in UCSC mm9 database (genome.ucsc.edu). A gene was designated as the target gene if the peak was present within 5000bp upstream of the transcription start site or inside of the gene.

For TCF1 (in mature CD8 T cells, accession number GSM1258235), we detected 591 significantly enriched regions (ranges between 104bp-1048bp, median: 233bp) by comparing it to control IgG using sorted post-select DP and $CD4^{+}8^{lo}$ thymocytes[1] (accession number GSM1258236). The detected regions could subsequently be mapped to 116 unique genes. For the two TCF1 experiments in murine thymocytes (GSM1285796 for TCF1-CAT and GSM1133644 for TCF1), we detected 732 (size ranges between 102bp-2632bp, median: 237bp), and 2600 (102bp-2632bp, median: 237bp) significant binding regions respectively after comparing to control TCF1-CAT-INPUT (GSM1285797) and TCF1-INPUT (GSM1133645) respectively. The detected regions could subsequently be mapped to respectively 131, and 653 unique genes (Table S2). The third analyzed ChIP-Seq data set was the binding of TCF7 (GSM773994). For TCF7 we detected 6395 significant binding regions (size ranges between 103bp-5840bp, median: 341bp) by comparing it to one control (input DNA of TCF7). These regions are subsequently mapped to 2015 genes (Table S2). The fourth public data set that we analyzed were three Beta-Catenin experiments, two with biotinylation and one based on FLAG-tag technology. As a background four different controls are used per experiment (2 with Beta-Catenin biotin without GSK and two GSK input samples). This resulted in respectively 990, 385, and 671 significant binding regions for Beta-Catenin-Biotin-rep1, Beta-Catenin-Biotin-rep2, and Beta-Catenin-Flag-rep1 and were mapped to 121, 49, and 79 genes (Table S2). Binding sites have median size of 336bp, 385bp, and 320bp.

To test the validity of the detected binding regions of each experiment, we expected an overrepresentation of WNT-associated genes. To test this, we overlaid the mapped genes with known WNT-associated genes (n=1136) from the Molecular Signature Database (MSigDB, v4.0), and detected that all seven ChIP-seq experiment showed a significant enrichment for binding in close vicinity of WNT-associated genes ($P \leq 0.05$, Table S1) based on the hypergeometric test. As an example, all seven experiments showed binding of in the transcriptional start site of *Axin2* (Figure S4A), whereas TCF1, and Beta-Catenin experiments showed also binding for *Lef1* (Figure S4A).

Pathway Analysis. Pathway analysis is performed by utilizing the Molecular Signature Database (MSigDB, v4.0) for the detection of enriched curated gene sets (C2), motif gene sets (C3), computational gene sets (C4), GO gene sets (C5), oncogenic signatures (C6), and immunologic signatures (C7). Gene sets and signatures are considered statistically significant when the P-value, derived from the hypergeometric test, is less or equal than 0.05 after correcting for multiple testing using Holm.

Mice

Mice were bred and maintained in the animal facilities of Leiden University Medical Center, in accordance with legal regulations in The Netherlands and with the approval of the Dutch animal ethical committee. C57Bl/6-CD45.1 (Ly5.1) and C57Bl/6-CD45.2 (Ly5.2) mice were obtained from the Jackson Laboratory. Mice

carrying targeted mutations on Apc were previously described (Fodde et al., 1994; Robanus-Maandag et al., 2010; Smits et al., 1999) and continuously backcrossed to C57Bl/6 background.

Flow Cytometry

The following antibodies were obtained from BD Biosciences (San Diego, CA): anti CD11b-PE (M1/70), anti CD19-APC (ID3) and anti CD117 (2B6). For Lineage depletion these markers were used: CD3 (145-2C11), CD4 (L3T4), CD8 (53-6.7), CD11b (M1/70), Gr1 (RB6-8C5), B220 (Ra3-6B2), Ter119 (Ly76) and Nk1.1 (PK136) biotin and subsequently were stained with streptavidin eFluor 450 (48-4317) from eBioscience. The following antibodies were also purchased from eBiosiences: B220 PE-Cy7 (RA3-6B2), Gr1 eFluor 450 (RB6-8C5) and Sca1 PE-Cy7 (D7). Cells were stained in Fluorescenceactivated cell sorter (FACS) buffer (PBS, 2% bovine serum albumin, 0.1% sodium azide) for 30 min at 4 °C. Ultimately, Cells were washed and measured either on a Canto I, or an Aria (BD Biosciences). Data were analyzed using FlowJo software (Tree Star, Ashland, OR, USA).

Prolferation, apoptosis and differentiation assays

5×10^4 sorted BM LSKs from APC WT and APC 15lox/15lox mice were transduced with titrated amount of CRE viruses in stemspan with FTS cytokines as previously described. For apoptosis assay harvested cells after 2 days (Day 0) or 5 days (Day 3) of culture, cells were stained with either 7AAD/AnnexinV (BD Bioscience), or PE-Active caspase-3 apoptosis kit (BD pharmingen) according to the manufacturer's instruction. For proliferation assay, cells were labelled with 5 uM Cell Proliferation Dye eFluor® 670 (eBioscience) at Day 0. Subsequently, cells were harvested at Day 3 and were assessed by flow cytometry for proliferation.

For differentiation assay 2×10^4 BM LSKs were used and transduced cells at Day 0 were transferred onto confluent monolayers of OP9 WT and cocultured for additional 14 days with AlphaMEM 10% FCS containing 50 ng/ml rmSCF, 10 ng/ml rmFlt3L and 10 ng/ml rmIL-7 (all cytokines from R&D). After 7 days cells were harvested and transferred onto new monolayer of OP9 cells, and half of the medium were replaced every 3-4 days. Finally, after 14 days of coculture cells were harvested and assessed by flow cytometry for B and myeloid lineage differentiation.

Supplemental Figure Legends

Suppl. Fig 1a: Validation of differential gene expression by Q-PCR. Sorted LSK cells were cultured and transduced with CRE-GFP as described in the supplemental experimental procedures. RNA was isolated and used for analysis by Q-PCR for the indicated Wnt target genes.
Suppl. Fig 1b: Biological processes associated with clusters 1 and 2. For details see text

Suppl. Fig 2: High Wnt signaling is associated with differentiation into monocytes and B lymphocytes based on published gene sets.

Suppl. Fig 3: No differences in apoptosis and cell cycle in high Wnt signature when compared to published gene sets.

Suppl. Fig 4a: Tcf and beta catenin binding sites in the Lef1 and Axin2 promoters based on literature data mining of CHIP-Seq data

Suppl. Fig 4b: Differentially expressed genes from the gene expression profiles of heterozygote samples against 1572T,1638N, and full KO, and detected in A. 157 differential expressed genes with $P<0.05$ and B. the representation of 55 unique gene sets (see also Table S3)

Figure S1

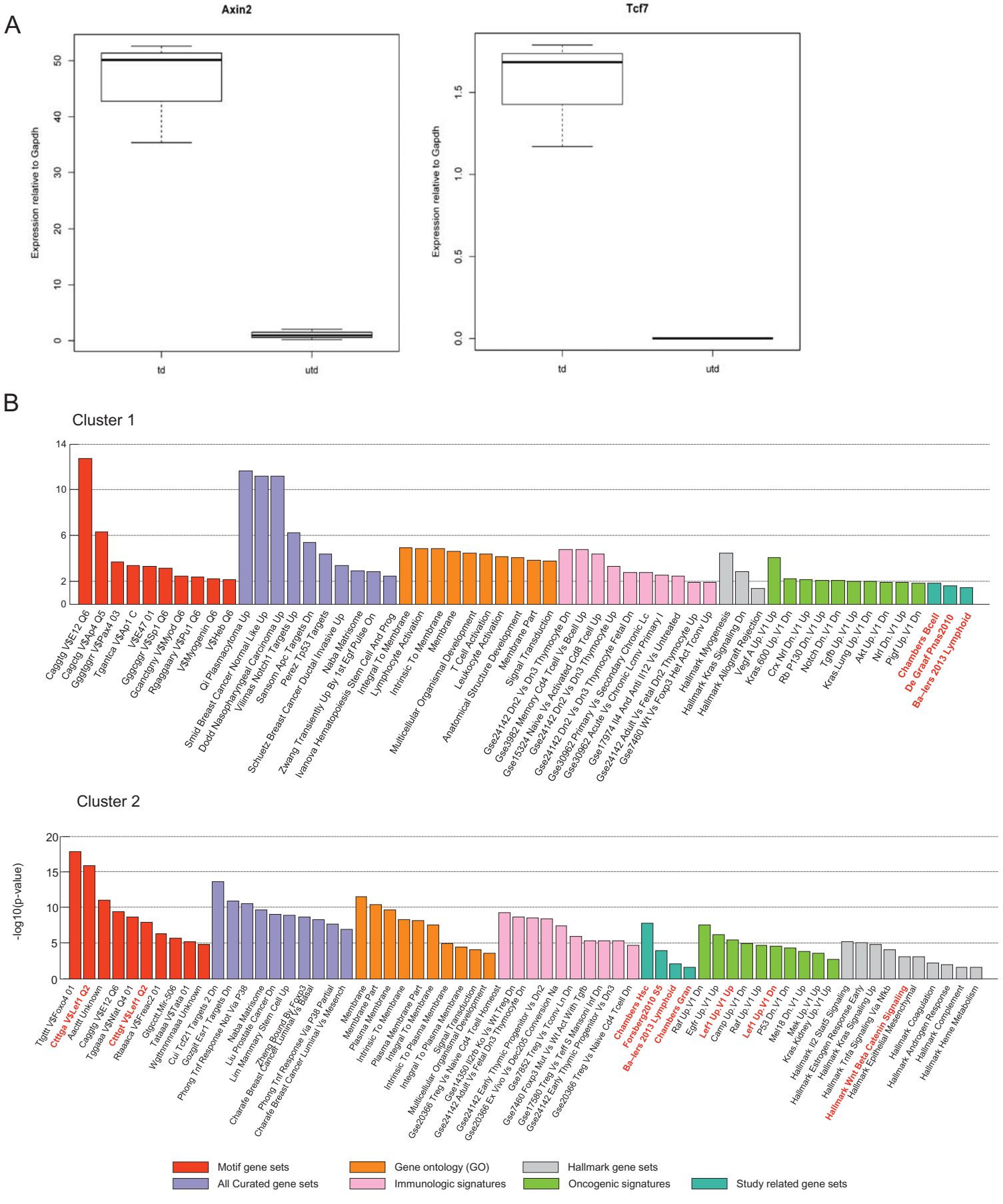
A
Axin2
Tcf7
Expression relative to Gapdh
td
utd
B
Cluster 1
Cluster 2
-log10(p-value)
Motif gene sets
All Curated gene sets
Gene ontology (GO)
Immunologic signatures
Hallmark gene sets
Oncogenic signatures
Study related gene sets

Figure S2

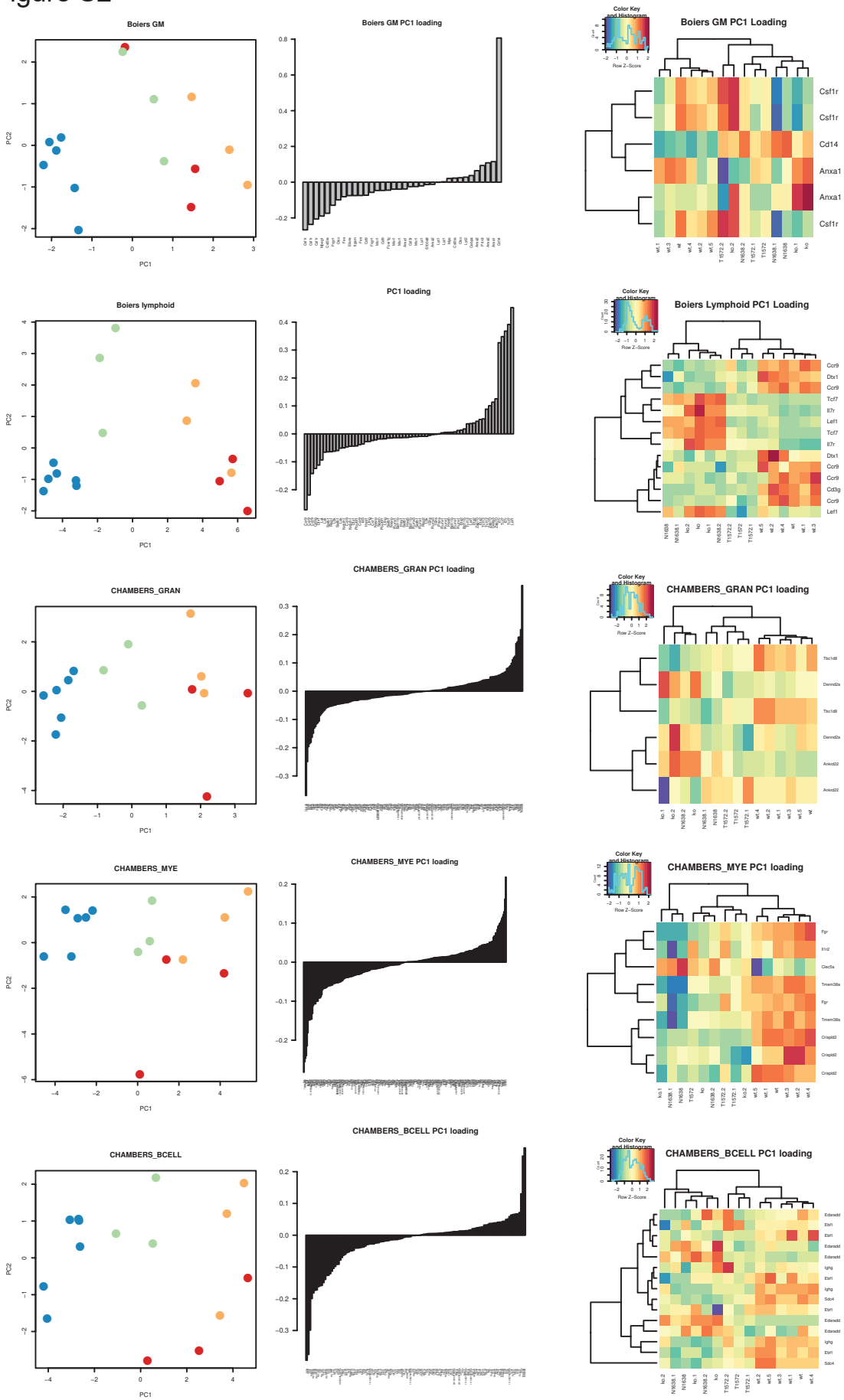

Differentiation signatures as determined by Boiers (Cell Stem Cell 2013) and Chambers (Cell Stem Cell 2007).

Stem cell signature, such as proposed by Ivanova (Science 2002), Forsberg (PLoS One 2010), Chambers (Cell Stem Cell 2007) and de Graaf (PNAS 2010) and Ridell (Cell 2014) were mostly driven by only a few genes.

Figure S3

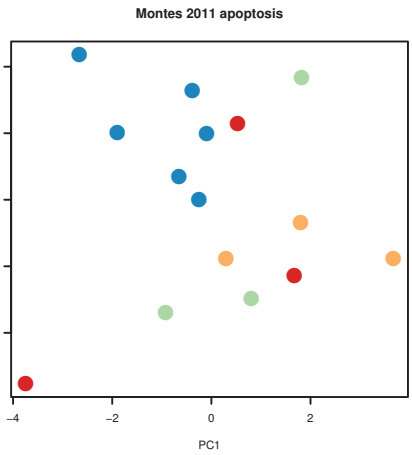
Montes 2011 apoptosis
PC1

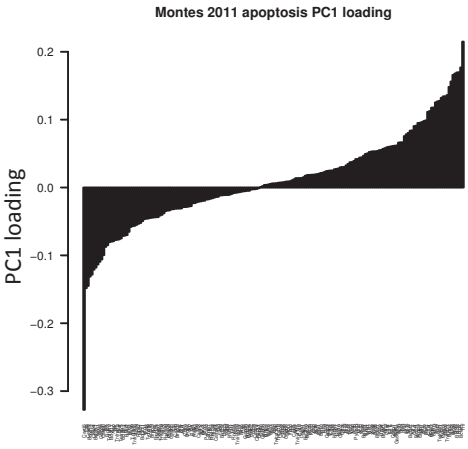
Montes 2011 apoptosis PC1 loading
PC1 loading

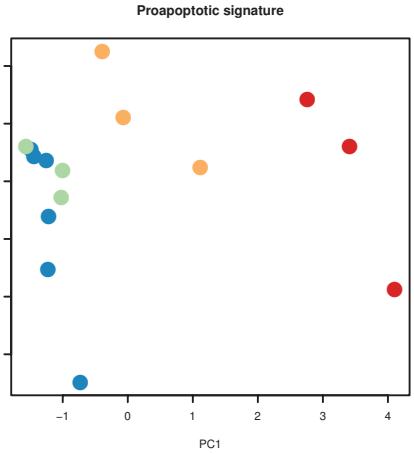
Proapoptotic signature
PC1

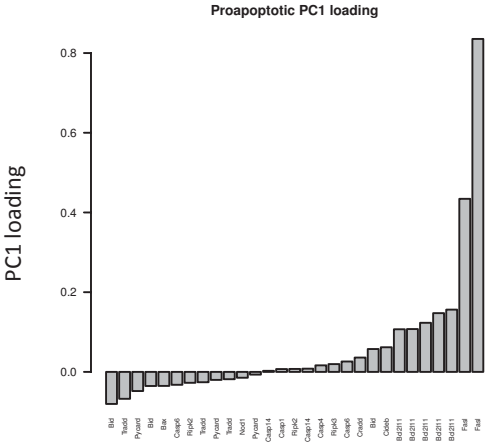
Proapoptotic PC1 loading
PC1 loading

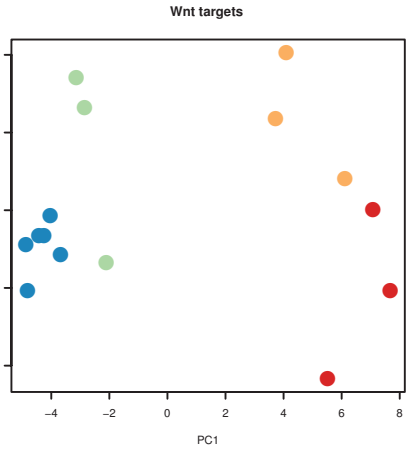
Wnt targets
PC1

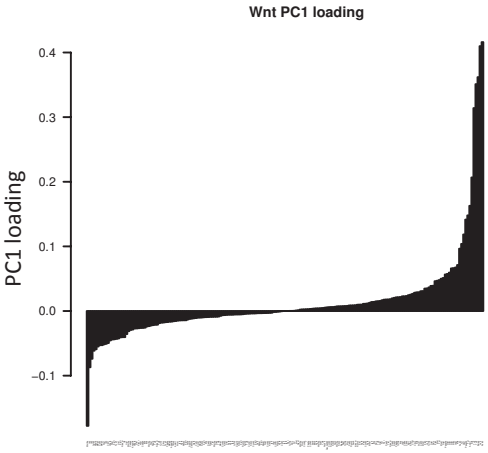
Wnt PC1 loading
PC1 loading

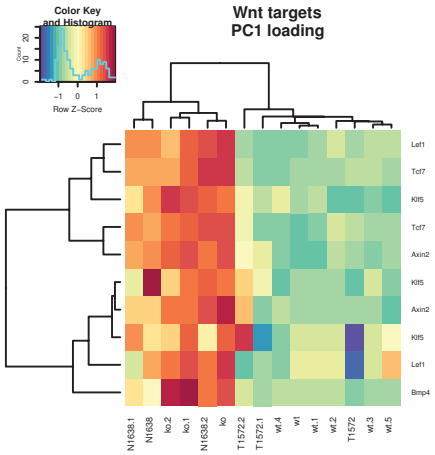
Color Key and Histogram
Row Z-Score
Wnt targets
PC1 loading
Lef1
Tcf7
Klf5
Tcf7
Axin2
Klf5
Axin2
Klf5
Lef1
Bmp4
N1638.1
N1638
ko.2
ko.1
N1638.2
ko
T1572.2
T1572.1
wt.4
wt
wt.1
wt.2
T1572
wt.3
wt.5

Figure S4

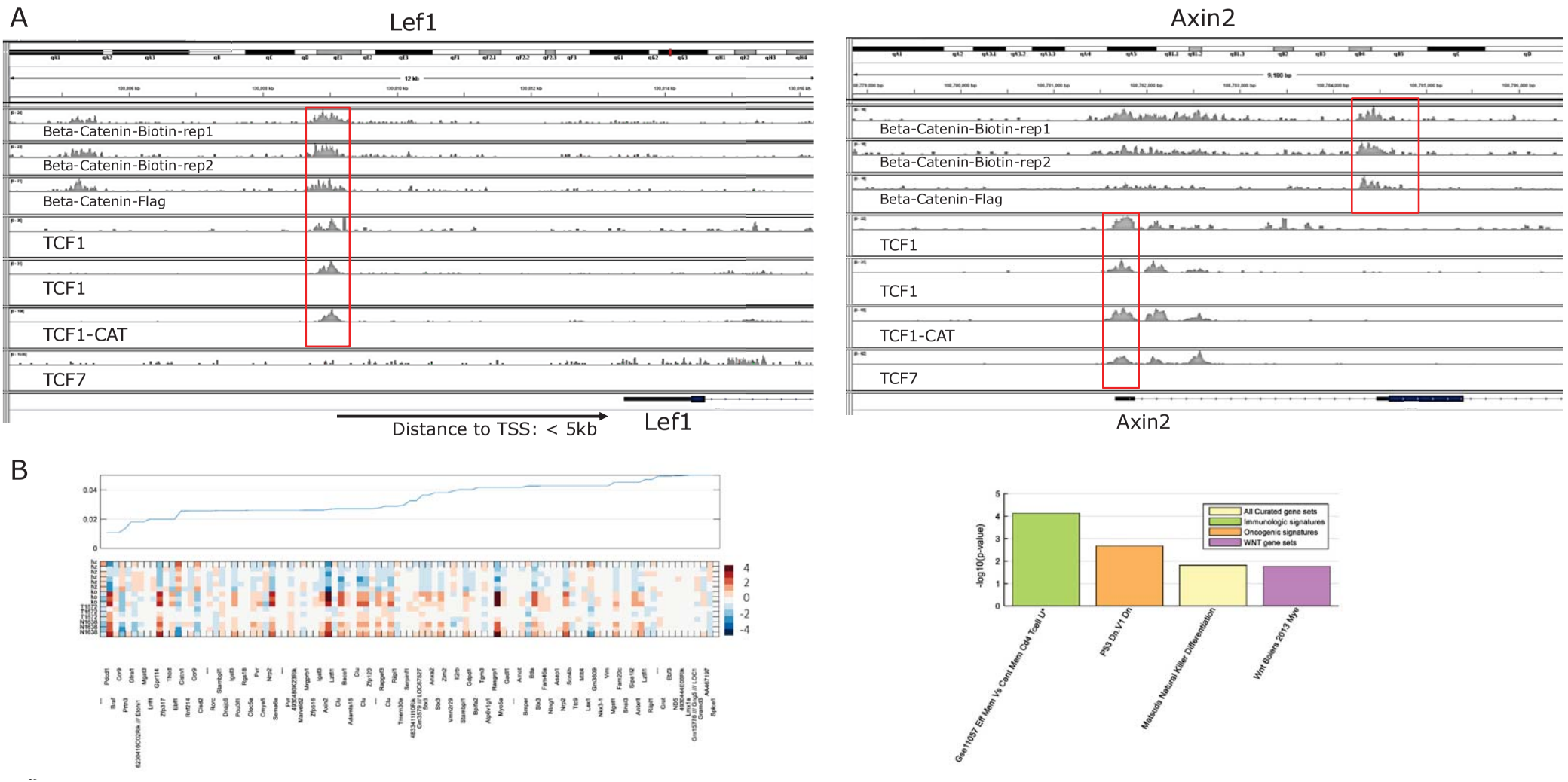
A
Lef1
Beta-Catenin-Biotin-rep1
Beta-Catenin-Biotin-rep2
Beta-Catenin-Flag
TCF1
TCF1
TCF1-CAT
TCF7
Distance to TSS: < 5kb
Lef1
Axin2
Beta-Catenin-Biotin-rep1
Beta-Catenin-Biotin-rep2
Beta-Catenin-Flag
TCF1
TCF1
TCF1-CAT
TCF7
Axin2
B
All Curated gene sets
Immunologic signatures
Oncogenic signatures
WNT gene sets
-log10(p-value)
Gse11057 Eff Mem Vs Cent Mem Cd4 Tcell U*
PS3 Dn.V1 Dn
Matsuzda Natural Killer Differentiation
Wnt Bioarx 2013 Mye

Table S1

Gene-set	Pathway	$P_{BY} \leq 0.05$	Genes
All Curated gene sets	MATSUDA_NATURAL_KILLER_DIFFERENTIATION	6.58E-06	ANXA1,APCDD1,CCR9,CD160,CDC23,GPR34,IL2RB,MYO5A,NTRK3,PDCD1,PLAGL1,PRSS23,PTPRF,PVR,SH3BGRL2,SYTL2,TCF7,TULP3,XCL1,ZC3H12C
All Curated gene sets	PICCALUGA_ANGIOIMMUNOBLASTIC_LYMPHOMA_UP	0.0002209	ANTXR1,CD93,CLU,DCLK1,FN1,FSTL1,IL18,LAMC1,PLA2G4C,RAI14,TMEM163,TNS1
All Curated gene sets	LIU_PROSTATE_CANCER_DN	0.0002209	BEND5,CHST2,CLU,CRISPLD2,EPAS1,GPR155,ITGA2,PHLDA1,PLAGL1,PRSS23,RHOJ,ROBO1,TFCP2L1,TMEM35,TNS1,WIF1,ZCCHC14
All Curated gene sets	ONDER_CDH1_TARGETS_2_DN	0.0002209	ALDH1A3,CD83,CDK5R1,EPAS1,FGD6,FST,GJB5,IGSF3,IL18,ITGA2,KLF5,PTPRF,ROBO1,TFCP2L1,THBD,TNFRSF25,TPD52L1
All Curated gene sets	DELYS_THYROID_CANCER_UP	0.0006965	ALDH1A3,ANXA1,CHST2,DPP4,ENTPD1,FN1,IGSF3,ITGA2,MED13,NRP2,NT5E,P4HA2,PRSS23,PTPRF,S100A5,STX3
All Curated gene sets	ST_WNT_BETA_CATENIN_PATHWAY	0.001009	APC,AXIN2,DKK2,FSTL1,NKD1,WIF1
All Curated gene sets	SANA_TNF_SIGNALING_DN	0.001009	ANTXR1,ANXA1,CLU,EPAS1,GIMAP6,NT5E,PHLDA1,RHOJ
All Curated gene sets	GOZGIT_ESR1_TARGETS_DN	0.001305	ABHD2,CLU,DCLK1,FETUB,GFRA1,GPC4,MB21D2,MYO5A,PPAP2A,PRSS23,RASGRP1,RNF144B,SDK1,SH3BGRL2,SHROOM3,SIPA1L2,SYTL2,THBD,THSD4
All Curated gene sets	CUI_TCF21_TARGETS_2_UP	0.001305	ANTXR1,APCDD1,ARSB,BMP4,BMPER,CLU,DCLK1,EMID1,FN1,GAS2L3,HUNK,KLF5,LYPD6B,NKD1,NRP2
All Curated gene sets	GAVIN_PDE3B_TARGETS	0.001305	ENTPD1,IL18,LAMC1,NT5E,SYTL2
All Curated gene sets	NABA_MATRISOME	0.003449	ADAM22,ANXA1,BMP4,BMPER,CRISPLD2,ELFN1,EMID1,FN1,FREM2,FST,FSTL1,GPC4,IL18,ISM1,KY,LAMC1,P4HA2,S100A5,SCUBE3,THSD4,WIF1,XCL1
All Curated gene sets	KEGG_WNT_SIGNALING_PATHWAY	0.00359	APC,AXIN2,CAMK2D,DKK2,LEF1,NFATC2,NKD1,TCF7,WIF1
All Curated gene sets	CERVERA_SDHB_TARGETS_1_UP	0.00359	CAND2,CCDC109B,FSTL1,IL18,LYPD6B,PACSIN1,PRSS23,TNFRSF19
All Curated gene sets	KINSEY_TARGETS_OF_EWSR1_FLI1_FUSION_DN	0.005222	CAMK2D,DCLK1,DLC1,FAM63A,FN1,FSTL1,LAMC1,MB21D2,NT5E,PHLDA1,PRSS23,SIPA1L2
All Curated gene sets	CHARAFE_BREAST_CANCER_LUMINAL_VS_BASAL_DN	0.005292	ADA,ALDH1A3,ANTXR1,ANXA1,CD14,FST,FSTL1,IL18,IL7R,KLF5,LAMC1,NT5E,PHLDA1,ZC3H12C
All Curated gene sets	RIGGI_EWING_SARCOMA_PROGENITOR_DN	0.007768	ABHD2,ALDH1A3,BACE1,BMP4,CLU,FST,NRP2,PHLDA1,TNFRSF19
All Curated gene sets	SANSOM_WNT_PATHWAY_REQUIRE_MYC	0.008652	AXIN2,LEF1,NKD1,TCF7,TNFRSF19,WIF1
All Curated gene sets	PASQUALUCCI_LYMPHOMA_BY_GC_STAGE_UP	0.008714	ADA,ANTXR1,ENTPD1,IRF4,NUDT4,OSBPL1A,PHLDA1,PVR,SH3BGRL2,SHROOM3,TULP3
All Curated gene sets	BYSTRYKH_HEMATOPOIESIS_STEM_CELL_QTL_TRANS	0.008714	AXIN2,CD14,CHST2,EFHD1,EXTL3,FAM63A,GFRA1,GPC4,IL2RB,KIF5C,LEF1,MYO5A,PDCD1,STX3,SULT1A1,TEK,TFCP2L1,THBD,TULP3,XCL1
All Curated gene sets	GAUSSMANN_MLL_AF4_FUSION_TARGETS_F_UP	0.009692	ARHGAP28,ARSB,BMP4,BMPER,FST,GPC4,IL18,NT5E,TEK
All Curated gene sets	GAVIN_FOXP3_TARGETS_CLUSTER_P4	0.01055	CCDC109B,CD83,EPAS1,IL2RB,LYPD6B,PLAGL1,SH3BGRL2
All Curated gene sets	KEGG_CYTOKINE_CYTOKINE_RECEPTOR_INTERACTION	0.01299	CCR2,CCR9,EDAR,IL17RB,IL18,IL2RB,IL7R,TNFRSF19,TNFRSF25,XCL1
All Curated gene sets	DODD_NASOPHARYNGEAL_CARCINOMA_UP	0.01525	ABHD2,ALDH1A3,ANXA1,APCDD1,ATP13A4,BACE1,BDH1,BEND5,CAND2,CLU,EDAR,EPAS1,FAM63A,FMN1,IL18,KLF5,LYPD6B,PRKAA2,PRSS23,SH3BGRL2,SMPD3,SNX31,SYTL2,TNFRSF19,TNS1,TUBB3
All Curated gene sets	CREIGHTON_ENDOCRINE_THERAPY_RESISTANCE_1	0.01646	BMPER,CCDC101,CRISPLD2,DLC1,EFHD1,FREM2,GFRA1,ITGA2,MB21D2,MYO5A,PRSS23,SYTL2,THSD4,TPD52L1
All Curated gene sets	SMID_BREAST_CANCER_NORMAL_LIKE_UP	0.01763	CCR2,CD3G,CLU,DPP4,GIMAP6,IL7R,LEF1,NT5E,SNCAIP,THBD,TNFRSF25,WIF1,XCL1
All Curated gene sets	SMIRNOV_CIRCULATING_ENDOTHELIOCYTES_IN_CANCER_UP	0.01851	B4GALT5,CD14,CD93,CLU,EPAS1,PRSS23,THBD,TNS1
All Curated gene sets	WALLACE_PROSTATE_CANCER_RACE_UP	0.01852	CCDC109B,CD83,CD93,CLU,DLC1,GIMAP6,IL7R,RASGRP1,THBD,TMEM35
All Curated gene sets	QI_PLASMACYTOMA_UP	0.02286	CARD11,CCR2,CD3G,CLU,DPP4,IL17RB,IL18,IL2RB,TUBB3,XCL1
All Curated gene sets	AMIT_EGF_RESPONSE_480_HELA	0.02337	ABHD2,DCLK1,FST,ITGA2,NUDT4,PTPRF,PVR,TUBB3
All Curated gene sets	NABA_MATRISOME_ASSOCIATED	0.03018	ADAM22,ANXA1,BMP4,ELFN1,FREM2,FST,FSTL1,GPC4,IL18,ISM1,KY,P4HA2,S100A5,SCUBE3,WIF1,XCL1
All Curated gene sets	REACTOME_IMMUNE_SYSTEM	0.03141	BTLA,CAMK2D,CARD11,CCR2,CD14,CD160,CD3G,CDC23,IL18,IL2RB,IL7R,IRF4,OSBPL1A,PDCD1,PVR,RAP1GAP2,RASGRP1,RNF144B
All Curated gene sets	FULCHER_INFLAMMATORY_RESPONSE_LECTIN_VS_LPS_UP	0.03141	ABHD2,CD93,CHST2,FN1,IL7R,IRF4,MB21D2,MYO5A,NRIP3,P4HA2,PHLDA1,RAI14,RASGRP1,THBD
All Curated gene sets	SCHAEFFER_PROSTATE_DEVELOPMENT_48HR_UP	0.03313	ALDH1A3,ANXA1,BDH1,CLU,CRISPLD2,EDARADD,GPR155,NT5E,PPFIBP2,SULT1A1,TFCP2L1,TPD52L1,WIF1
All Curated gene sets	KIM_MYC_AMPLIFICATION_TARGETS_DN	0.03336	DCLK1,GAS2L3,IL17RB,KLF5,NFATC2,SHROOM3
All Curated gene sets	LIM_MAMMARY_STEM_CELL_UP	0.04392	ANTXR1,EDARADD,EPAS1,FST,ISM1,LAMC1,NRP2,NT5E,PPAP2A,RHOJ,THSD1,TNS1,WIF1
All Curated gene sets	KEGG_BASAL_CELL_CARCINOMA	0.04862	APC,AXIN2,BMP4,LEF1,TCF7
All Curated gene sets	TAKEDA_TARGETS_OF_NUP98_HOXA9_FUSION_8D_DN	0.04862	ANTXR1,CD14,CLU,ENTPD1,EPAS1,GPR34,IL7R,TMEM163
All Curated gene sets	LINDGREN_BLADDER_CANCER_CLUSTER_2B	0.0488	CRISPLD2,EFHD1,ENTPD1,IL7R,LEF1,MYO5A,NRP2,TBC1D8,TCF7,THBD,TNS1
All Curated gene sets	NUYTTEN_EZH2_TARGETS_UP	0.0488	ANXA1,AXIN2,B4GALT5,BACE1,CCDC109B,CD83,FGD6,FN1,GPR155,NT5E,P4HA2,PLAGL1,PRRG1,PTPRF,ROBO1,STX3,TCF7,THSD1,ZC3H12C
All Curated gene sets	SCHAEFFER_PROSTATE_DEVELOPMENT_48HR_DN	0.0488	ANTXR1,CD83,CHDH,DKK2,GAS2L3,HUNK,LYPD6B,NRP2,P4HA2,PRTG,RHOJ,SIPA1L2
Computational gene sets	MODULE_46	2.83E-06	ADA,CCR2,CCR9,CD14,CD3G,CD83,CDK5R1,CLU,DPP4,ENTPD1,FN1,IL18,IL2RB,IL7R,P4HA2,PDCD1,XCL1
Computational gene sets	MODULE_75	2.83E-06	ADA,CCR2,CCR9,CD14,CD3G,CD83,CDK5R1,CLU,DPP4,FN1,IL18,IL2RB,IL7R,P4HA2,PDCD1,TEK,XCL1
Gene ontology (GO)	PLASMA_MEMBRANE_PART	0.000438	ACTN2,APC,BACE1,CACNA1B,CACNA1D,CARD11,CCR2,CCR9,CD160,CD83,DCLK1,ENTPD1,GPC4,GPR34,IL17RB,IL2RB,ITGA2,NTRK3,PRRG1,PTPRF,ROBO1,SHROOM3,STX3,SYTL2,TEK,THBD,TNFRSF25
Gene ontology (GO)	MEMBRANE	0.0006684	ACTN2,APC,BACE1,CACNA1B,CACNA1D,CARD11,CCR2,CCR9,CD14,CD160,CD83,CDK5R1,DCLK1,ENTPD1,GPC4,GPR114,GPR34,IL17RB,IL2RB,ITGA2,NTRK3,PLA2G4C,PPAP2A,PRRG1,PTPRF,PVR,RNF144B,ROBO1,SHROOM3,SLC7A4,STX3,SYTL2,TBC1D8,TEK,THBD,TNFRSF25
Gene ontology (GO)	PLASMA_MEMBRANE	0.0007698	ACTN2,APC,BACE1,CACNA1B,CACNA1D,CARD11,CCR2,CCR9,CD14,CD160,CD83,DCLK1,ENTPD1,GPC4,GPR34,IL17RB,IL2RB,ITGA2,NTRK3,PPAP2A,PRRG1,PTPRF,ROBO1,SHROOM3,STX3,SYTL2,TEK,THBD,TNFRSF25
Gene ontology (GO)	MEMBRANE_PART	0.001722	ACTN2,APC,BACE1,CACNA1B,CACNA1D,CARD11,CCR2,CCR9,CD160,CD83,DCLK1,ENTPD1,GPC4,GPR114,GPR34,IL17RB,IL2RB,ITGA2,NTRK3,PRRG1,PTPRF,PVR,RNF144B,ROBO1,SHROOM3,SLC7A4,STX3,SYTL2,TEK,THBD,TNFRSF25
Gene ontology (GO)	SIGNAL_TRANSDUCTION	0.007247	ANXA1,AXIN2,CCR2,CCR9,CD14,CD160,CD3G,CD83,CDK5R1,DLC1,EDARADD,EPAS1,FGD6,GPR34,HUNK,IL2RB,IL7R,KCNIP2,MED13,NTRK3,NUDT4,PPAP2A,PRKAA2,PTPRF,RASGRP1,TEK,TNFRSF25,TPD52L1,XCL1
Gene ontology (GO)	RESPONSE_TO_EXTERNAL_STIMULUS	0.01613	AHSG,ANXA1,CCR2,CCR9,CHST2,ENTPD1,ITGA2,PGLYRP2,SHROOM3,THBD,XCL1
Gene ontology (GO)	RECEPTOR_ACTIVITY	0.01613	CD14,CD160,CD3G,GFRA1,GPR114,IL2RB,IL7R,MED13,NRP2,PGLYRP2,PTPRF,PVR,ROBO1,TEK,TNFRSF25
Hallmark gene sets	HALLMARK_ESTROGEN_RESPONSE_EARLY	0.004103	ABHD2,DLC1,FAM63A,GFRA1,IL17RB,PRSS23,RASGRP1,THSD4,TPD52L1
Hallmark gene sets	HALLMARK_INFLAMMATORY_RESPONSE	0.006397	CD14,CHST2,IL18,IL2RB,IL7R,PVR,RASGRP1,RNF144B
Hallmark gene sets	HALLMARK_COAGULATION	0.006397	ANXA1,CLU,DPP4,FN1,ITGA2,PRSS23,THBD
Hallmark gene sets	HALLMARK_IL2_STAT5_SIGNALING	0.006397	CD83,IL2RB,IRF4,NT5E,PHLDA1,PLAGL1,PPAP2A,SH3BGRL2
Hallmark gene sets	HALLMARK_WNT_BETA_CATENIN_SIGNALING	0.01107	AXIN2,LEF1,NKD1,TCF7
Hallmark gene sets	HALLMARK_COMPLEMENT	0.01636	ACTN2,CDK5R1,CLU,DPP4,FN1,KCNIP2,RASGRP1
Immunologic signatures	GSE20366_EX_VIVO_VS_DEC205_CONVERSION_NAIVE_CD4_TCELL_UP	0.001054	ACTN2,CCR2,CD160,EPAS1,GPR114,GPR34,IL17RB,RASGRP1,THBD,XCL1,XKRX
Immunologic signatures	GSE24142_EARLY_THYMIC_PROGENITOR_VS_DN2_THYMOCYTE_DN	0.001054	ADA,AXIN2,CCDC109B,CD3G,DPP4,EDARADD,IL17RB,IL7R,PDCD1,PTPRF,TUBB3
Immunologic signatures	GSE7852_TREG_VS_TCONV_LN_UP	0.001054	CCR2,CD83,ENTPD1,FGD6,IRF4,LAMC1,NT5E,PLAGL1,PPAP2A,ZC3H12C,ZDHHC23
Immunologic signatures	GSE10325_LUPUS_CD4_TCELL_VS_LUPUS_BCELL_UP	0.003344	ANXA1,CCDC109B,CD3G,DPP4,GIMAP6,IL7R,LEF1,TCF7,TNFRSF25,ZCCHC14
Immunologic signatures	GSE30962_PRIMARY_VS_SECONDARY_CHRONIC_LCMV_INF_CD8_TCELL_	0.003344	AHSG,ANXA1,CD93,ENTPD1,EPAS1,GPR114,GPR34,PRKAA2,RASGRP1,TMEM163
Immunologic signatures	GSE24142_EARLY_THYMIC_PROGENITOR_VS_DN2_THYMOCYTE_ADULT_	0.003403	AXIN2,CCDC109B,CD3G,EDARADD,IL17RB,IL7R,LEF1,PPAP2A,PTPRF,SYTL2
Immunologic signatures	GSE7460_TCONV_VS_TREG_LN_DN	0.004089	CD83,DPP4,ENTPD1,IL2RB,IRF4,NT5E,PPAP2A,SH3BGRL2,ZC3H12C,ZDHHC23
Immunologic signatures	GSE20366_EX_VIVO_VS_DEC205_CONVERSION_NAIVE_CD4_TCELL_DN	0.0137	ANXA1,CCDC109B,CD83,DCLK1,IL18,PLAGL1,RNF144B,SNX31,STX3
Immunologic signatures	GSE10325_CD4_TCELL_VS_BCELL_UP	0.01559	ANXA1,CCR2,CD3G,DPP4,GIMAP6,IL2RB,LEF1,RASGRP1,TNFRSF25
Immunologic signatures	GSE24142_EARLY_THYMIC_PROGENITOR_VS_DN3_THYMOCYTE_DN	0.01559	ADA,CCDC109B,GFRA1,IL7R,LEF1,PDCD1,PTPRF,TUBB3,TULP3
Immunologic signatures	GSE39820_CTRL_VS_IL1B_IL6_IL23A_CD4_TCELL_UP	0.01559	CD83,GAS2L3,GPR34,LYPD6B,PACSIN1,PHLDA1,PLAGL1,RASGRP1,SYTL2
Immunologic signatures	GSE7460_TCONV_VS_TREG_THYMUS_DN	0.01559	CCDC109B,CD83,IGSF3,IL2RB,KIF5C,NRP2,PLAGL1,PPAP2A,SH3BGRL2
Immunologic signatures	GSE7852_TREG_VS_TCONV_THYMUS_UP	0.01634	CCDC109B,CCR2,CD83,IGSF3,KIF5C,PDCD1,PLAGL1,PPAP2A,SH3BGRL2
Immunologic signatures	GSE24142_DN2_VS_DN3_THYMOCYTE_DN	0.01649	CCR9,CD3G,GFRA1,IRF4,LEF1,PHLDA1,PTPRF,TBC1D8,TULP3
Immunologic signatures	GSE3982_BCELL_VS_CENT_MEMORY_CD4_TCELL_DN	0.03801	DLC1,DPP4,IL7R,ITGA2,PHLDA1,PRKAA2,TCF7,TNS1
Immunologic signatures	GSE3982_MEMORY_CD4_TCELL_VS_BCELL_UP	0.04586	ANXA1,CAND2,CD3G,DPP4,GIMAP6,IL2RB,KIF5C,PHLDA1
Motif gene sets	TTGTTT_V$FOXO4_01	0.0001493	ANXA1,APC,AXIN2,BDH1,BMP4,CCDC109B,CD83,DLC1,EDAR,ENTPD1,EXTL3,FAM63A,FN1,FST,FSTL1,GFRA1,IL18,IL7R,IRF4,ITGA2,KCNIP2,KLF5,LAMC1,NKD1,NRP2,NTRK3,RNF214,ROBO1,SCUBE3,SDK1,SMPD3,SNCAIP,SYTL2,TEK,TNFRSF19,XKRX,ZCCHC14
Motif gene sets	CTTTGA_V$LEF1_Q2	0.0001493	ABHD2,ATP13A4,BACE1,CD160,CPB1,DLC1,EMID1,FAM63A,FST,GFRA1,GPC4,KIF7,KY,LEF1,MB21D2,MED13,NKD1,NRP2,ROBO1,SESTD1,SLC22A23,SNCAIP,SYTL2,TBC1D8,TCF7,TNFRSF19,XKRX
Motif gene sets	TGGAAA_V$NFAT_Q4_01	0.006435	ANTXR1,B4GALT5,BMP4,CHDH,DCLK1,DKK2,DLC1,EFHD1,FN1,FST,FSTL1,GALNT7,IGSF3,IL17RB,IL7R,IRF4,ITGA2,KCNIP2,KLF5,MED13,NFATC2,SCUBE3,SH3BGRL2,SMPD3,SNCAIP,TBC1D8,TMEM163,TMEM35,TNFRSF19,TNS1,XKRX
Motif gene sets	V$TCF4_Q5	0.009151	ABHD2,FAM63A,FST,GPC4,KY,NKD1,NRP2,SYTL2,TCF7,TNFRSF19
Oncogenic signatures	CAMP_UP.V1_DN	1.97E-05	ANXA1,BACE1,CAMK2D,CCR9,CD160,CD83,CHST2,FSTL1,IL7R,NFATC2,TUBB3,ZCCHC14
Oncogenic signatures	MEL18_DN.V1_UP	0.03587	CD83,CHST2,CRISPLD2,IL7R,NRP2,NT5E,TEK

Table S2				
Experiment	**Study**	**Significantly detected binding regions**	**Mapped to genes within 5Kb from TSS**	**P-value, Significance with WNT-associated genesets from MsigDB**
TCF1	GSE52070	591	116	0.033
TCF1 (n=2)	GSE46662	732 in Sample 1	131	0.050
		2600 in Sample 2	653	9.395E-04
TCF7	GSE31221	6395	2015	0.017
Beta-Catenin (n=3)	GSE43565	990 in Sample 1	121	2.273E-04
		385 in Sample 2	49	9.564E-04
		671 in Sample 3	79	0.004

Table S3

Gene-set	Pathway	$P_{BY} \leq 0.05$	Genes
WNT gene sets	WNT_BOIERS_2013_LYMPHOID	0.01053	CCR9,LEF1,TCF7
All Curated gene sets	ST_WNT_BETA_CATENIN_PATHWAY	0.0001483	APC,AXIN2,DKK2,FSTL1,NKD1,WIF1
All Curated gene sets	RIGGI_EWING_SARCOMA_PROGENITOR_DN	0.0006029	ALDH1A3,BACE1,BMP4,CLU,EBF1,FST,NRP2,PHLDA1,TNFRSF19
All Curated gene sets	SANSOM_WNT_PATHWAY_REQUIRE_MYC	0.001274	AXIN2,LEF1,NKD1,TCF7,TNFRSF19,WIF1
All Curated gene sets	LIU_PROSTATE_CANCER_DN	0.001855	BEND5,CHST2,CLU,EPAS1,ITGA2,NDNF,PHLDA1,PRSS23,ROBO1,TFCP2L1,WIF1,ZCCHC14
All Curated gene sets	MATSUDA_NATURAL_KILLER_DIFFERENTIATION	0.001855	ANXA1,APCDD1,CCR9,CD160,EBF1,NTRK3,PDCD1,PRSS23,SH3BGRL2,TCF7,TULP3,ZC3H12C
All Curated gene sets	KINSEY_TARGETS_OF_EWSR1_FLII_FUSION_DN	0.001979	DCLK1,EBF1,FAM63A,FSTL1,IL17RD,MB21D2,NT5E,PHLDA1,PRSS23,SIPA1L2
All Curated gene sets	KUMAR_TARGETS_OF_MLL_AF9_FUSION	0.001979	ANXA1,CCR9,CD83,EBF1,EXTL3,GPC4,IL7R,IRF4,LEF1,TCF7,TNFRSF19
All Curated gene sets	CUI_TCF21_TARGETS_2_UP	0.003067	ANTXR1,APCDD1,ARSB,BMP4,CLU,DCLK1,HUNK,KLF5,LYPD6B,NKD1,NRP2
All Curated gene sets	CHARAFE_BREAST_CANCER_LUMINAL_VS_BASAL_DN	0.003672	ADA,ALDH1A3,ANTXR1,ANXA1,FST,FSTL1,IL7R,KLF5,NT5E,PHLDA1,ZC3H12C
All Curated gene sets	DODD_NASOPHARYNGEAL_CARCINOMA_UP	0.003672	ALDH1A3,ANXA1,APCDD1,ATP13A4,BACE1,BDH1,BEND5,CLU,EBF1,EDAR,EPAS1,FAM63A,KLF5,LYPD6B,PRKAA2,PRSS23,SH3BGRL2,TNFRSF19,TUBB3,UST,WWC1
All Curated gene sets	DELYS_THYROID_CANCER_UP	0.003672	ALDH1A3,ANXA1,CHST2,DPP4,IGSF3,ITGA2,MED13,NRP2,NT5E,PRSS23,STX3
All Curated gene sets	ONDER_CDH1_TARGETS_2_DN	0.004116	ALDH1A3,CD83,EPAS1,FST,IGSF3,ITGA2,KLF5,ROBO1,TFCP2L1,THBD,WWC1
All Curated gene sets	SANA_TNF_SIGNALING_DN	0.004116	ANTXR1,ANXA1,CLU,EPAS1,NT5E,PHLDA1
All Curated gene sets	KEGG_WNT_SIGNALING_PATHWAY	0.004871	APC,AXIN2,DKK2,LEF1,NKD1,TCF7,WIF1
All Curated gene sets	KEGG_BASAL_CELL_CARCINOMA	0.005932	APC,AXIN2,BMP4,LEF1,TCF7
All Curated gene sets	CUI_TCF21_TARGETS_2_DN	0.006368	ANXA1,ARHGAP28,BACE1,DKK2,DPP4,EBF1,EPAS1,MED13,NT5E,PPAP2A,SH3BGRL2,SHROOM3,SNCAIP,THBD
All Curated gene sets	BYSTRYKH_HEMATOPOIESIS_STEM_CELL_QTL_TRANS	0.01287	AXIN2,CHST2,EFHD1,EXTL3,FAM63A,GPC4,KIF5C,LEF1,PDCD1,STX3,SULT1A1,TFCP2L1,THBD,TULP3
All Curated gene sets	GAUSSMANN_MLL_AF4_FUSION_TARGETS_F_UP	0.0141	ARHGAP28,ARSB,BMP4,FST,GPC4,IL17RD,NT5E
All Curated gene sets	CHARAFE_BREAST_CANCER_LUMINAL_VS_MESENCHYMAL_DN	0.01879	ANTXR1,ANXA1,CHST2,FST,FSTL1,IL7R,NT5E,PHLDA1,RAI14,ZC3H12C
All Curated gene sets	GOZGIT_ESR1_TARGETS_DN	0.03962	CLU,DCLK1,FETUB,GPC4,MB21D2,PPAP2A,PRSS23,RASGRP1,SH3BGRL2,SHROOM3,SIPA1L2,THBD
All Curated gene sets	ENK_UV_RESPONSE_EPIDERMIS_DN	0.04184	ANXA1,APC,CD83,ITGA2,PHLDA1,PPAP2A,PRSS23,RAI14,ROBO1,THBD
All Curated gene sets	WNT_SIGNALING	0.04194	APC,LEF1,NKD1,TCF7,WIF1
All Curated gene sets	PID_PS1_PATHWAY	0.04605	APC,DKK2,NKD1,WIF1
All Curated gene sets	SENESE_HDAC1_AND_HDAC2_TARGETS_UP	0.04605	DCLK1,DKK2,EXTL3,IL7R,NRIP3,PHLDA1,WWC1
All Curated gene sets	KIM_MYC_AMPLIFICATION_TARGETS_DN	0.04605	DCLK1,IL17RB,IL17RD,KLF5,SHROOM3
Motif gene sets	TTGTTT_V$FOXO4_01	3.15E-05	ANXA1,APC,AXIN2,BDH1,BMP4,CCDC109B,CD83,EBF1,EDAR,EXTL3,FAM63A,FST,FSTL1,IL7R,IRF4,ITGA2,KCNIP2,KLF5,NKD1,NRP2,NTRK3,RNF214,ROBO1,SNCAIP,TNFRSF19,XKRX,ZCCHC14
Motif gene sets	CTTTGA_V$LEF1_Q2	0.0003071	ATP13A4,BACE1,CD160,CPB1,FAM63A,FST,GPC4,KY,LEF1,MB21D2,MED13,NKD1,NRP2,ROBO1,SLC22A23,SNCAIP,TCF7,TNFRSF19,XKRX
Motif gene sets	CAGGTG_V$E12_Q6	0.001973	ACTN2,AXIN2,BACE1,BMP4,CD83,CPB1,EBF1,EDAR,EPAS1,EXTL3,FST,IGSF3,ITGA2,KCNIP2,LEF1,LYPD6B,MB21D2,NRIP3,NRP2,NTRK3,SH3BGRL2,SNCAIP,TCF7,UNC45B,UST,WWC1
Motif gene sets	V$TCF4_Q5	0.005048	FAM63A,FST,GPC4,KY,NKD1,NRP2,TCF7,TNFRSF19
Motif gene sets	TGGAAA_V$NFAT_Q4_01	0.006748	ANTXR1,BMP4,DCLK1,DKK2,EBF1,EFHD1,FST,FSTL1,IGSF3,IL17RB,IL7R,IRF4,ITGA2,KCNIP2,KLF5,MED13,SH3BGRL2,SNCAIP,TMEM163,TNFRSF19,XKRX
Motif gene sets	TATTATA,MIR-374	0.01408	ARHGAP28,BACE1,CHST2,EDAR,MED13,RNF214,UST,ZCCHC14
Motif gene sets	TGCCAAR_V$NF1_Q6	0.01468	AHSG,AXIN2,DCLK1,KY,LEF1,MB21D2,MED13,NRP2,NTRK3,RAI14,ROBO1,XKRX
Motif gene sets	RTAAACA_V$FREAC2_01	0.02911	AXIN2,BMP4,FST,FSTL1,IRF4,KY,NTRK3,ROBO1,SNCAIP,TCF7,TNFRSF19,UNC45B,UST
Oncogenic signatures	CAMP_UP.V1_DN	5.78E-06	ANXA1,BACE1,CCR9,CD160,CD83,CHST2,FSTL1,IL7R,TUBB3,ZCCHC14
Oncogenic signatures	AKT_UP.V1_DN	0.04519	AXIN2,EDARADD,TNFRSF19,TULP3,WIF1,ZC3H12C
Immunologic signature	GSE24142_EARLY_THYMIC_PROGENITOR_VS_DN2_THYMOCYTE_DN	0.001121	ADA,AXIN2,CCDC109B,DPP4,EDARADD,IL17RB,IL7R,PDCD1,TUBB3
Immunologic signature	GSE20366_EX_VIVO_VS_DEC205_CONVERSION_NAIVE_CD4_TCELL_UP	0.007534	ACTN2,CD160,EPAS1,GPR114,IL17RB,RASGRP1,THBD,XKRX
Immunologic signature	GSE10325_LUPUS_CD4_TCELL_VS_LUPUS_BCELL_UP	0.01556	ANXA1,CCDC109B,DPP4,IL7R,LEF1,TCF7,ZCCHC14
Immunologic signature	GSE14350_IL2RB_KO_VS_WT_TREG_DN	0.01556	CCDC109B,CD160,CD83,KY,NT5E,PDCD1,ZC3H12C
Immunologic signature	GSE24142_EARLY_THYMIC_PROGENITOR_VS_DN3_THYMOCYTE_DN	0.01556	ADA,CCDC109B,IL7R,LEF1,PDCD1,TUBB3,TULP3
Immunologic signature	GSE24142_EARLY_THYMIC_PROGENITOR_VS_DN2_THYMOCYTE_ADULT_DN	0.01556	AXIN2,CCDC109B,EDARADD,IL17RB,IL7R,LEF1,PPAP2A
Immunologic signature	GSE26495_NAIVE_VS_PD1HIGH_CD8_TCELL_UP	0.01556	BDH1,BEND5,EDAR,EFHD1,LEF1,NT5E,PPAP2A
Immunologic signature	GSE26495_NAIVE_VS_PD1LOW_CD8_TCELL_UP	0.01556	BDH1,BEND5,EDAR,EFHD1,LEF1,NT5E,PPAP2A
Immunologic signature	GSE30962_PRIMARY_VS_SECONDARY_CHRONIC_LCMV_INF_CD8_TCELL_DN	0.01556	AHSG,ANXA1,EPAS1,GPR114,PRKAA2,RASGRP1,TMEM163
Immunologic signature	GSE3982_BCELL_VS_CENT_MEMORY_CD4_TCELL_DN	0.01556	DPP4,IL7R,ITGA2,NDNF,PHLDA1,PRKAA2,TCF7
Immunologic signature	GSE7460_TCONV_VS_TREG_LN_DN	0.01556	CD83,DPP4,IRF4,NT5E,PPAP2A,SH3BGRL2,ZC3H12C
Immunologic signature	GSE7460_TCONV_VS_TREG_THYMUS_DN	0.01556	CCDC109B,CD83,IGSF3,KIF5C,NRP2,PPAP2A,SH3BGRL2
Immunologic signature	GSE7852_TREG_VS_TCONV_THYMUS_UP	0.01556	CCDC109B,CD83,IGSF3,KIF5C,PDCD1,PPAP2A,SH3BGRL2
Hallmark gene sets	HALLMARK_WNT_BETA_CATENIN_SIGNALING	0.002609	AXIN2,LEF1,NKD1,TCF7
Hallmark gene sets	HALLMARK_COAGULATION	0.002609	ANXA1,CLU,DPP4,ITGA2,PRSS23,THBD
Hallmark gene sets	HALLMARK_IL2_STAT5_SIGNALING	0.007102	CD83,IRF4,NT5E,PHLDA1,PPAP2A,SH3BGRL2
Hallmark gene sets	HALLMARK_KRAS_SIGNALING_DN	0.007102	CHST2,CPB1,EDAR,EFHD1,PDCD1,TFCP2L1
Hallmark gene sets	HALLMARK_ESTROGEN_RESPONSE_EARLY	0.04111	FAM63A,IL17RB,PRSS23,RASGRP1,WWC1
Hallmark gene sets	HALLMARK_COMPLEMENT	0.04111	ACTN2,CLU,DPP4,KCNIP2,RASGRP1